A THRUST ANEMOMETER FOR THE MEASUREMENT OF THE TURBULENT WIND VECTOR

Gerard J. McNally

New York University
Bronx, New York

January 1970

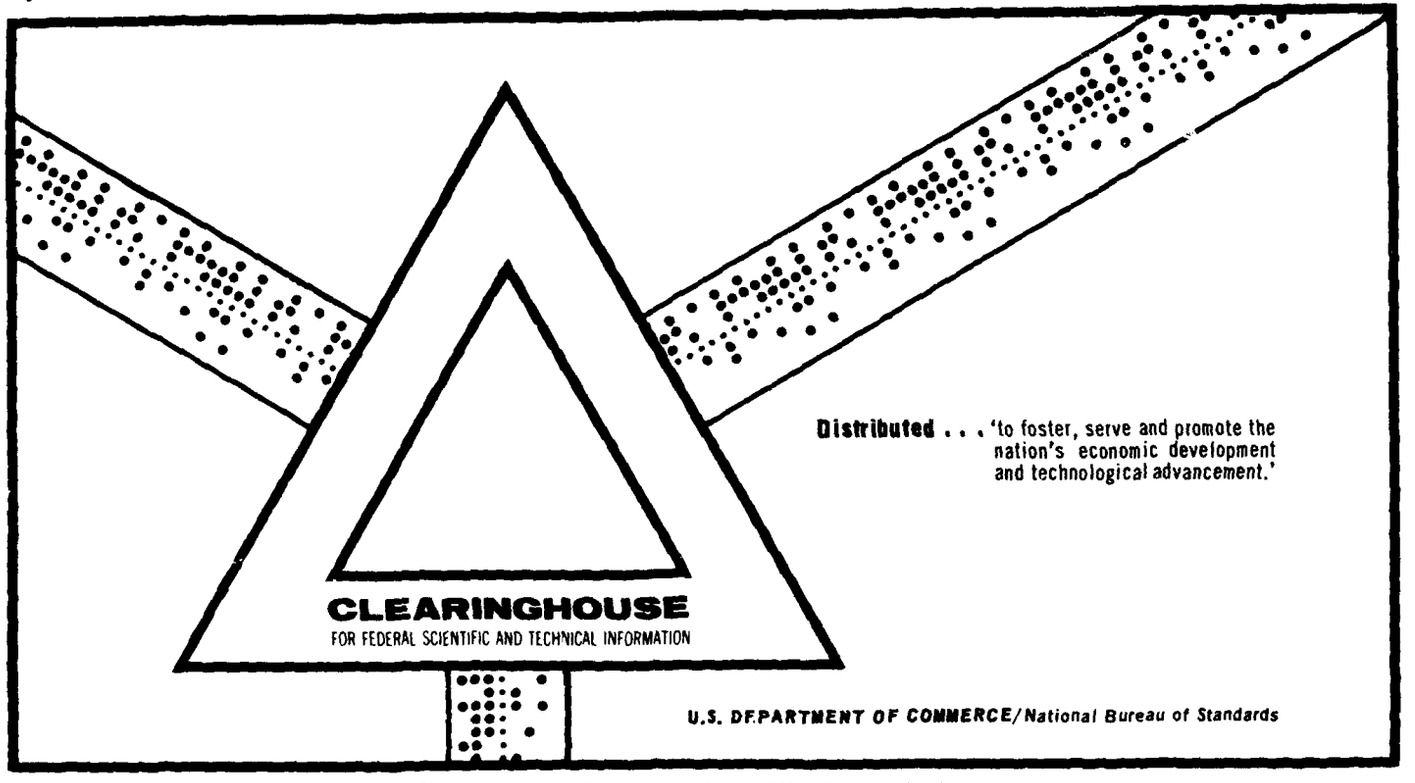

A THRUST ANEMOMETER FOR THE MEASUREMENT OF THE TURBULENT WIND VECTOR

By

Gerard J. McNally

January 1970

New York University
School of Engineering and Science
University Heights, New York, N.Y. 10453
Geophysical Sciences Laboratory TR-70-1
Department of Meteorology and Oceanography
Research Division

New York University
School of Engineering and Science
Department of Meteorology and Oceanography

Geophysical Sciences Laboratory TR-70-1

A THRUST ANEMOMETER FOR THE MEASUREMENT OF THE TURBULENT WIND VECTOR

By

Gerard J. McNally

Prepared for

Office of Naval Research

under

Contract Nonr 285(57)

January 1970

Table of Contents

List of Figures

List of Figures (continued)

Abstract

An improved version of a three component thrust anemometer is discussed in this paper. The design criteria and specifications of its component parts are outlined. Results of laboratory and wind tunnel tests are described which were designed to test the static characteristics and frequency response of the anemometer as well as results of wind tunnel tests. These tests demonstrate the anemometers adherence to the V^2 law ($\vec{F} = K \vec{V}_1 \vec{V}^1$) over the velocity range 0 to 25 miles per hour. Rotation tests performed at various wind speeds provide information on the anemometer's ability to resolve the vector wind into its components.

I. Introduction

An understanding of the mechanism of the turbulent exchange of energy across the air-sea boundary has been pursued for many years. One of the principal areas of investigation has been the exchange of momentum at this interface. This investigation of the turbulent exchange of momentum requires a special type of anemometry. The most straightforward method of determining the vertical flux of horizontal momentum is to measure the instantaneous horizontal and vertical velocity components separately, and thus determine the Reynolds stresses directly. The anemometry required for such measurements must be capable of measuring each of the three components of vector wind accurately over the frequently range of interest. In recent years these measurements have been attempted with several different type of anemometers, including heated films (R.W. Stewart and R.W. Burling, 1963), sonic (M. Miyake, 1965) and, heated thermistors with bi-vane (Pandolfo, 1960). These measurements have been made with varying degrees of success.

Among the most recent developments in turbulence anemometry is the three component thrust or drag sphere anemometer developed by E.A. L. Doe at New York University in 1963. A modified version of this anemometer was used in an air-sea boundary investigation (Kirwan, Adelfang, McNally, 1966). Still another version is currently in use at the Bedford Institute of Oceanography for a similar study (Smith, 1966). These anemometers performed satisfactorily, but as with all new instruments had a great deal of room for improvement. The drag sphere anemometer reported

on here is the result of an effort to provide that improvement and to produce a version of the thrust anemometer suitable for the aforementioned measurements.

II. Description of the Anemometer

The drag sphere anemometer consists of two units: the wind unit and the electronics unit. These units can be separated by as much as 500 feet with little or no deteriortation in performance. The wind unit contains the perforated styrofoam sphere sensor and five differential transformer transducers. The drag force exerted on the sphere is a function of velocity according to the relationship:

$$\vec{F} = K |\vec{V}| \vec{V}$$

where

$\vec{F}$ = force vector

$\vec{V}$ = wind vector

K = constant of proportionality

$$K = \frac{1}{2} \rho A C_D$$

where

ρ = density of gas

A = surface area of the sphere

C_D = drag coefficient of the sphere

The vector force exerted on the sphere is resolved into its components by means of the arrangement of the five rods supporting the sphere. The force components ultimately are sensed as displacements of the support

rods which are terminated in springs. The five support rods are arranged with three in the horizontal plane and two in the vertical. Each rod passed through a differential transformer which converts its displacement into changes in output voltage level. These output voltages are a linear function of displacement and thus the components of the drag force. The output voltages are brought to the electronics unit by means of an interconnecting cable. This cable also carries the required D.C. voltage excitation to the differential transformers from the power supply in the electronics unit.

The electronics unit consists of an operational amplifier for each of the three axis, summing networks for the transverse and vertical axis and regulated power supplied. Two transducers are used in the vertical and transverse axes so that the "common mode" output which results when a force is exerted on the third axis may be cancelled. A complete description of the theory and operation of the thrust anemometer is contained in a technical report by Kirwan, et al., 1966.

Two years of extensive testing coupled with field operations produced enough enthusiasm and confidence in the basic concepts of the anemometer to warrant the fabrication of the improved version reported on in this paper.

III. Design Criteria

Stability and operational simplicity were the prime design consideration of the new instrument. The instabilities in the original units both in the mechanical parts of the wind unit (springs, transducers, and dash pots) and the electronic components was one of the problems encountered in field operation. These instabilities, coupled with the inability to check and

adjust the instrument after it had been mounted and installed,represented the most serious operational problems.

A new type spring was the starting point in the design of the new anemometer. The spring constant plus the displacement range of the transducers, $\pm$ 0.05 inches, determine the maximum wind the anemometer can measure. Having fixed the spring constant, the minimum detectable wind speed is then determined by the amplifier gain and signal to noise ratio of the anemometer plus recording equipment. Therefore, in selecting a new spring constant, there has to be a compromise between range and resolution. The original units were designed to measure wind speeds to 60 miles per hour. Field operations showed 30 miles per hour to be a more realistic upper limit. Thus, the springs chosen were considerably softer than the original units with a deflection of 0.001 inches per gram of load as opposed to 0.0004 inches per gram of load. In addition to changing the spring constant a more rugged spring was employed. The original cantelevered hairsprings were replaced by a larger corrogated spring of berrilium copper. The corrugations serve the dual purpose of strengthening the spring and keeping its deflection coaxial with the exciting force through its specified range of deflection. This latter aspect improved the linearity of the transducer output voltage versus exciting force. The springs proved to be linear over the range of $\pm$ 0.05 inches, the full travel of the transducer. The springs were stopped by means of nuts placed on the support rods (see Figure 3.1) to insure that the linearity would not be destroyed by overstressing them accidently.

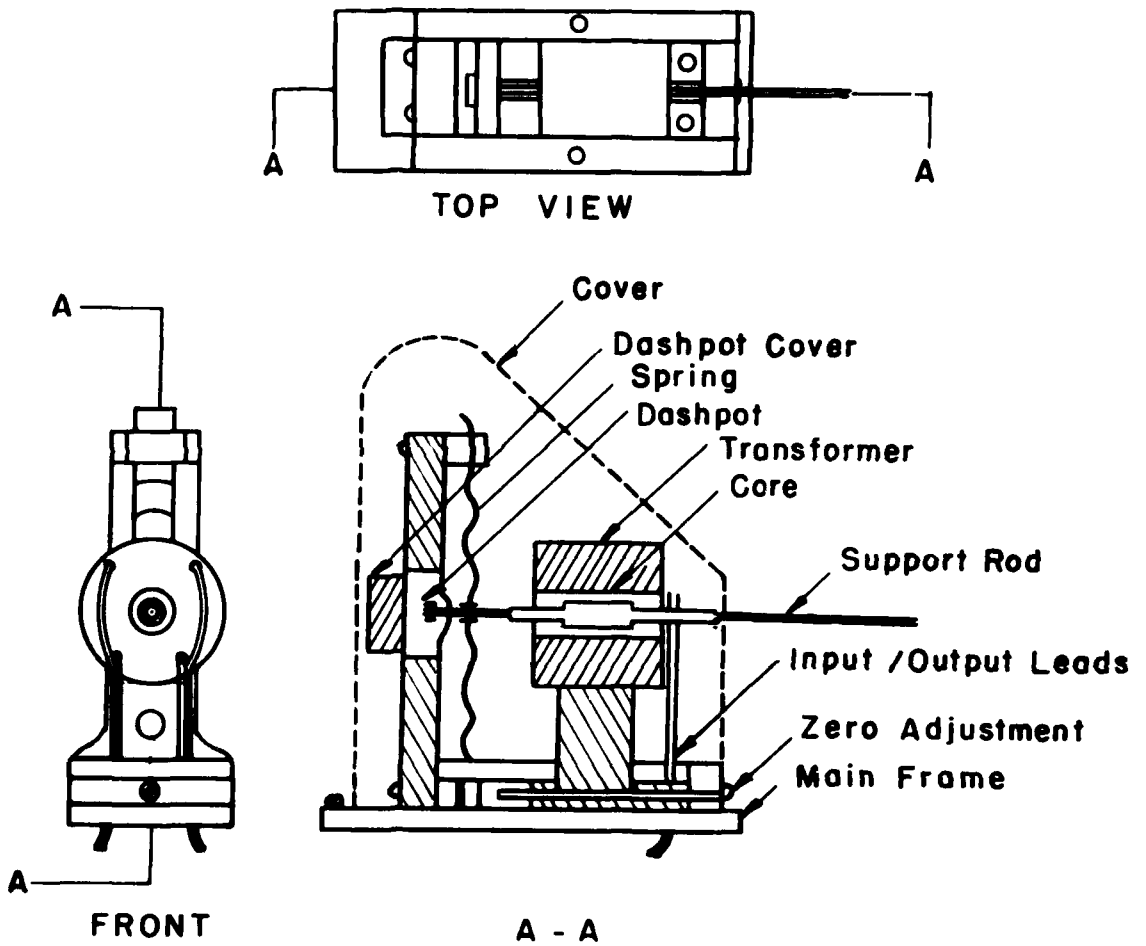

Figure 3.1. Differential transformer assembly

The dashpots in the original unit were simply annular openings in the rear support member of the transducer (see Figure 3.2). Each support rod was terminated in a brass slug or piston. The clearance between the piston and the walls of the annular opening was then filled with viscous oil to provide viscous shear-damping. However, the cantelevered springs did not insure a coaxial deflection of the rod and piston so that the pistons would tend to bind on the walls of dash pots resulting in sticking and hysterises. In order to prevent this and also to prevent the rapid loss of fluid, the dash pot arrangement was changed. An actual well was constructed in the rear support members of the transducers. The support rod terminated within the well. A small nut is attached to the end of the support rod. The well is filled with the silicon oil used as dash pot fluid and the cover screwed on. This arrangement has worked very well. It is easy to fill and when the need arises easy to empty. These features were especially useful when determining the proper viscosity silicon oil to use to optimize the frequency response. (See Section IV).

The electronics unit was completely redesigned so as to include the following: self contained regulated power supplies, choppter stabilized operational amplifiers, zero offset controls and x-axis zero-suppression. See Figures 3.3 to 3.6.

The self contained power supplies provide the necessary $\pm$ 15 volts DC for the operational amplifiers and the 6 volts DC required by the differential transformers. The supplies are designed to operate from a normal 115 volts AC, 60 hertz power line. They incorporate regulating circuitry so as to operate with variations in the power line voltage from 105 to 130

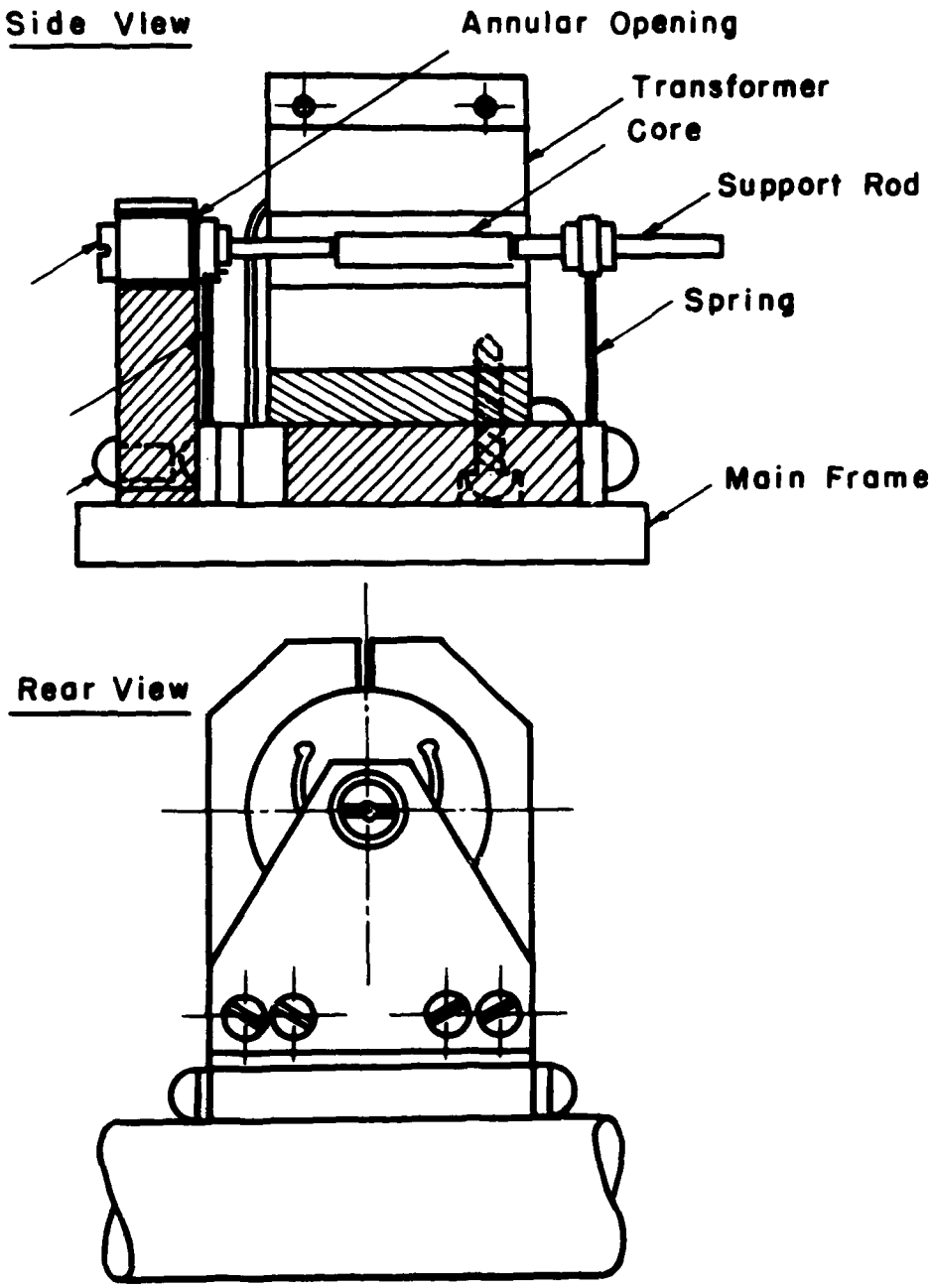

Figure 3.2. Differential transformer assembly - original unit.

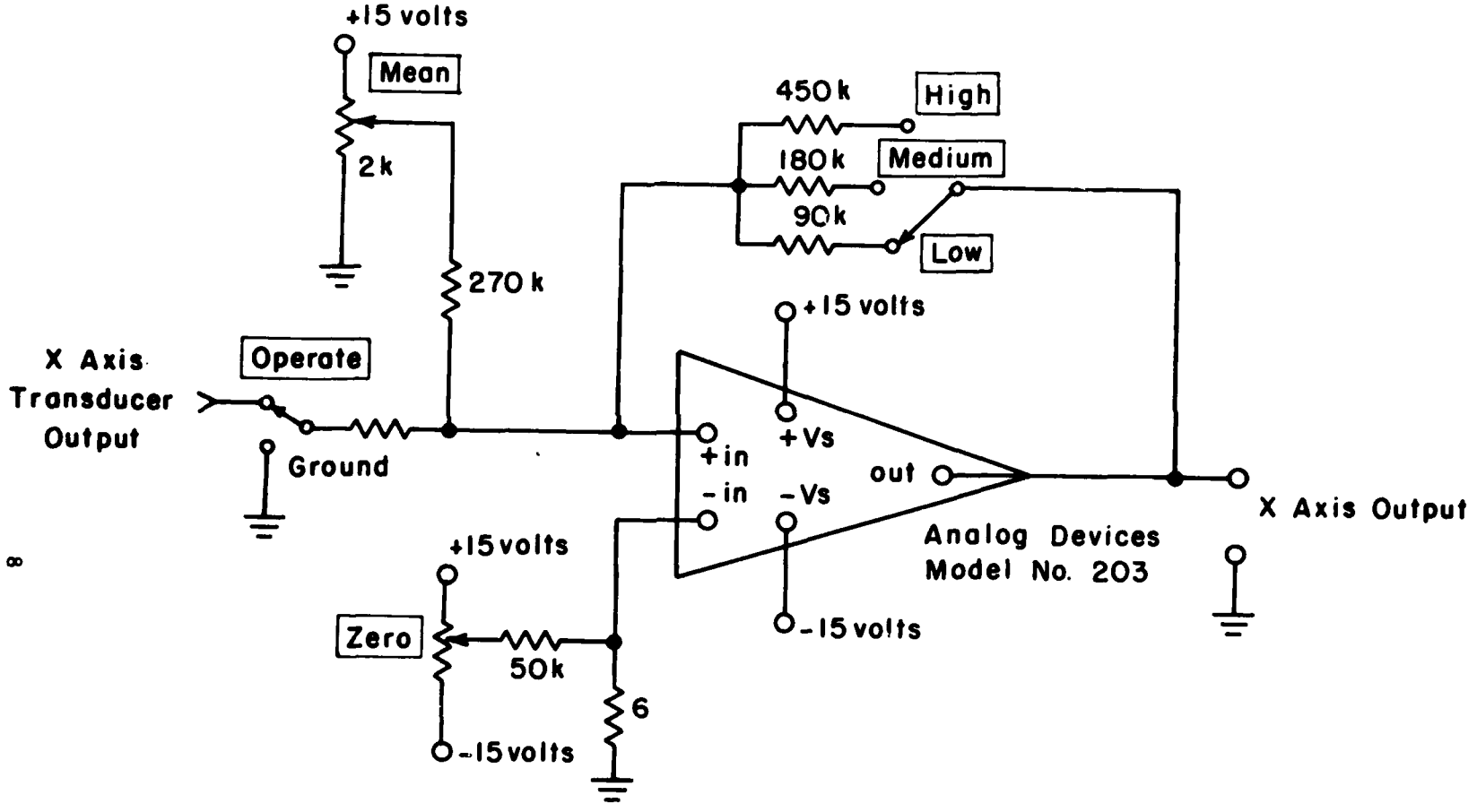

Figure 3.3. Simplified schematic of the X axis amplifier.

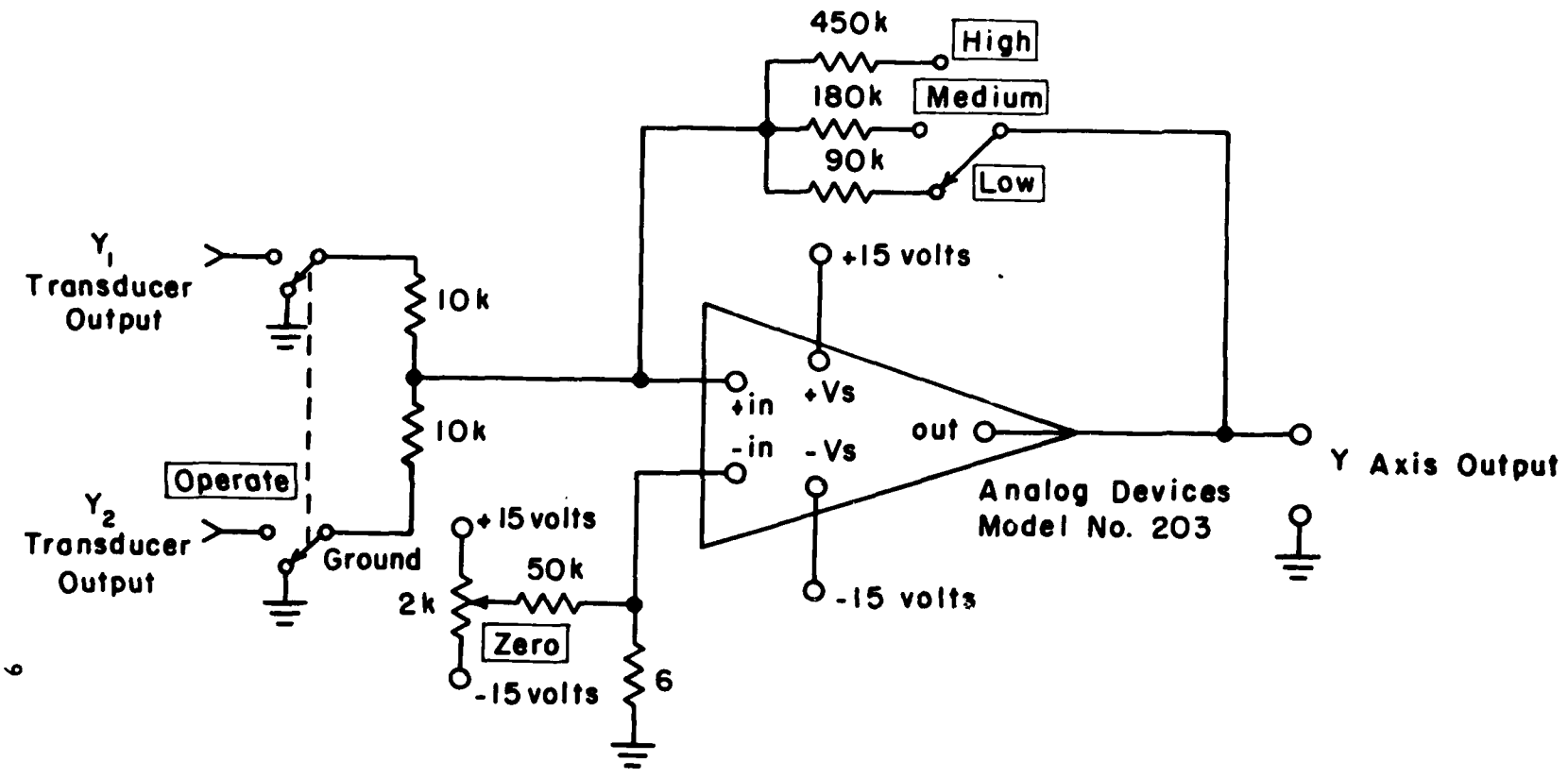

Figure 3.4. Simplified schematic of the Y (or Z) axis amplifier.

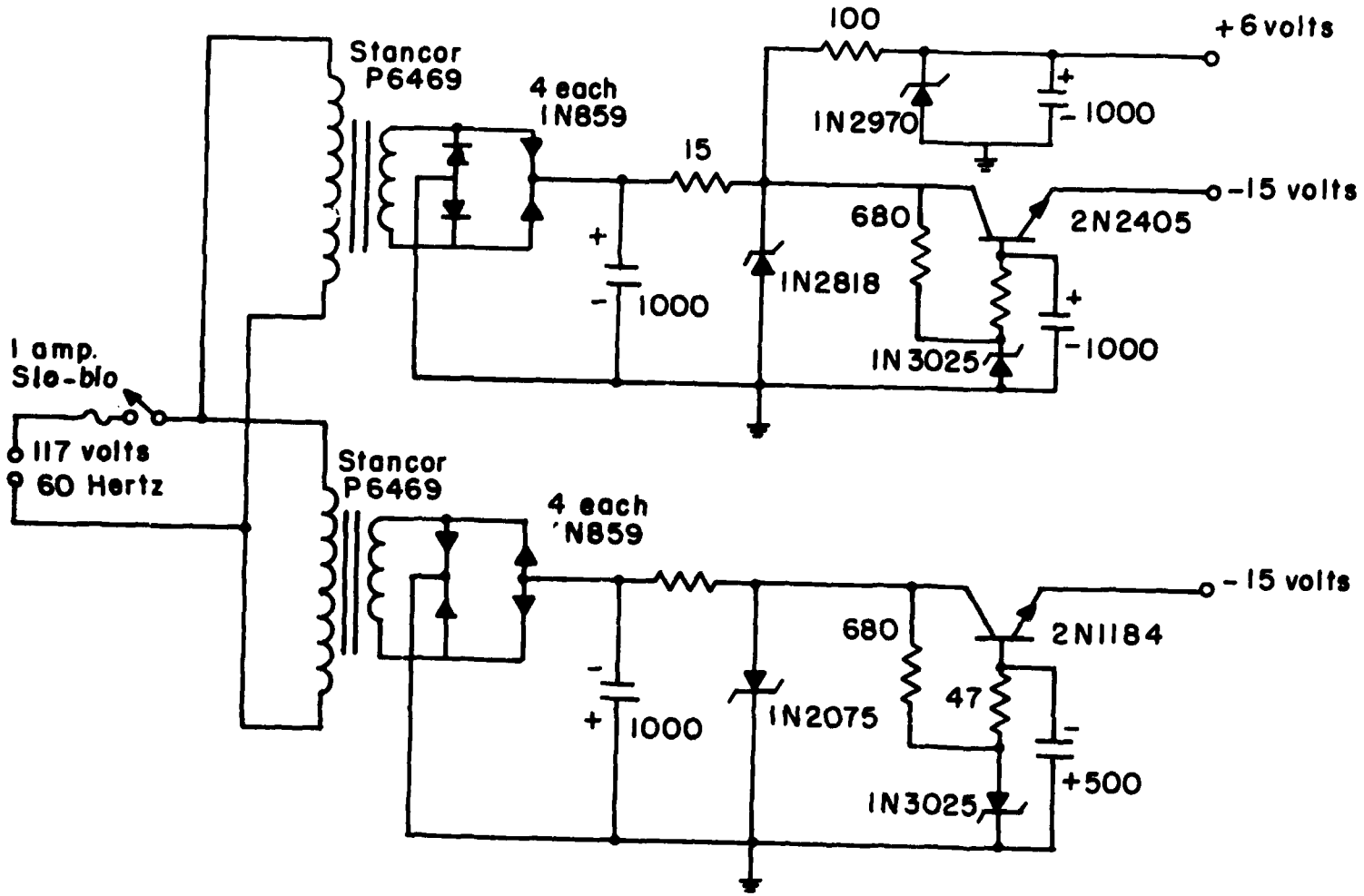

Figure 3.5. Power supply schematic.

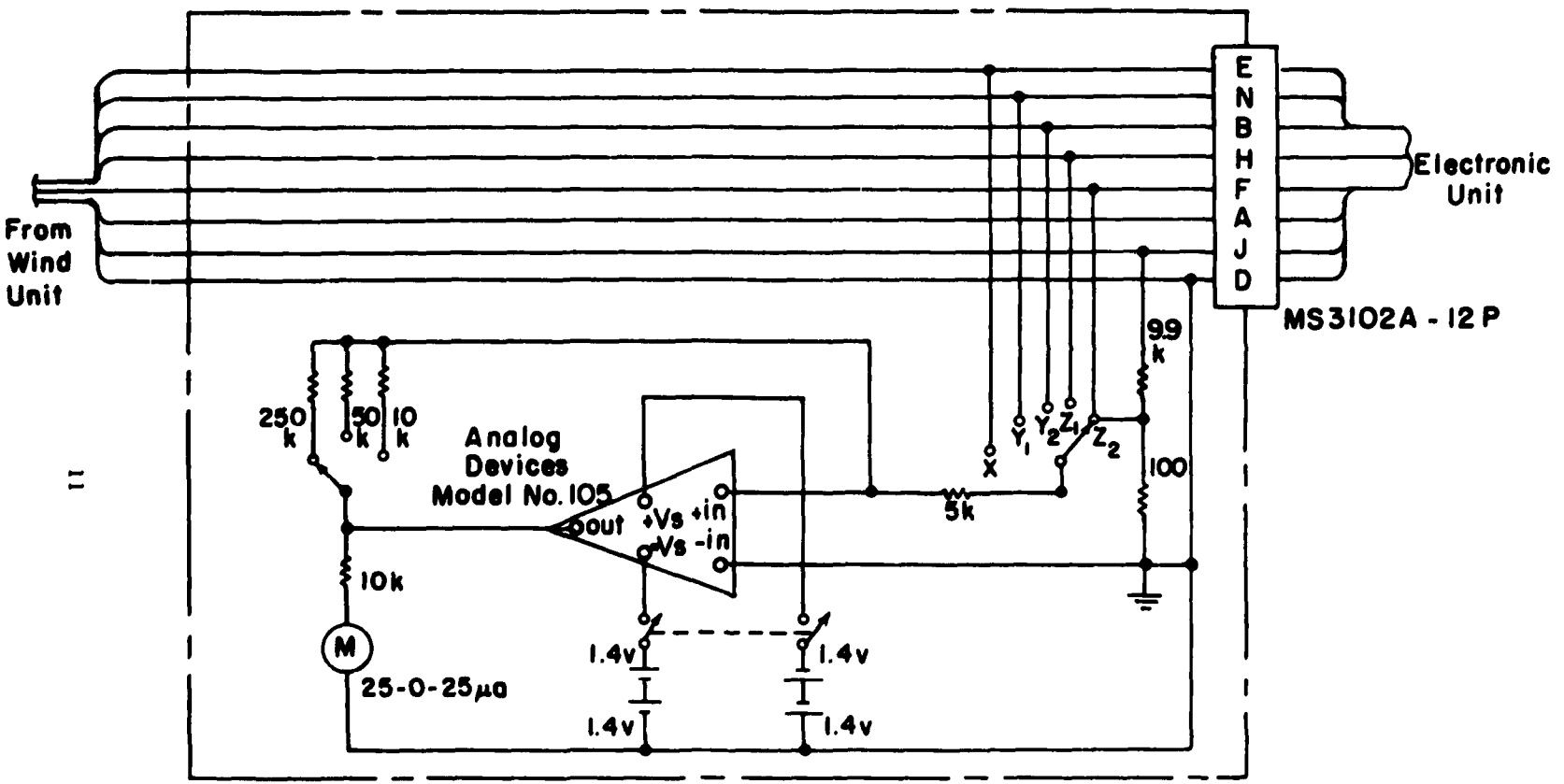

Figure 3.6. Test jig schematic.

volts. In addition, the output voltages of the supplies are very heavily filtered to reduce power supply "hum" to a minimum.

One of the most chronic problems encountered in field operations with the original units was drift in the operational amplifiers due to environmental temperature variations. Chopper stabilized amplifiers were substituted for the original amplifiers resulting in an order of magnitude improvement in temperature stability. The stability of the new unit is further enhanced by the lower gain requirements resulting from the choice of softer springs. A maximum gain (from transducer output of anemometer output) of approximately 90 is now required on the most sensitive range as compared to a gain of 1000 on the original units. An "Operate-Ground" switch was added so that drift in the amplifiers could be checked during operation. This switch disconnects the transducer signals from the input of the operational amplifiers and instead returns them to ground through their input resistors. This operation can be performed on any one of the three switch selected gain settings and allows the detection of changes in the output signals due to instabilities in the amplifiers since their inputs are grounded.

Zero controls were added and mounted on the front panel. These controls, one for each amplifier, allow the input signal to the amplifier to be offset a small amount to compensate for the small residual signals that might be present after the transducers have been set. Thus, the anemometer output signals are set to zero under a zero wind condition. These same controls also allow for corrections that might be needed to compensate for drift on the operational amplifiers.

In operation, the X-axis of the wind unit is aligned so as to be in the direction of the wind. Under this condition, the X-axis output voltage will contain a large mean component plus smaller variations, whereas the Y- and Z-axes output voltages will be approximately zero centered. This would severely limit the resolution of the X-axis output, since the gain would have to be such as to prevent the large mean signal from saturating the amplifier. In order to provide comparable resolution in all three axis, a "mean suppression" circuit was added. This circuit allows the mean signal to be "bucked out" at the input to the amplifier, and thus only the perturbating signals are amplified. A ten-turn heliput with a turns counting dial is provided on the front panel to adjust the mean suppression. The dial is turned until the X-axis output voltage is approximately zero-centered and the gain can then be increased. Figure 3.7 is a plot of dial reading versus output voltage. The mean voltage that has been suppressed is read from this plot; corrected for gain setting and then be added later in the data reduction process.

To complete the design, a method of checking and adjusting the transducers after the wind unit was installed had to be devised. A hood for the wind unit had been supplied with the original units. This hood was designed so as to enclose the entire wind unit (see Figure 3.8). Unfortunately, a hood of this size created such a drag force that the instrument would vibrate quite violently in even light winds. These vibrations created so much noise at the output that it was impossible to check the transducer settings.

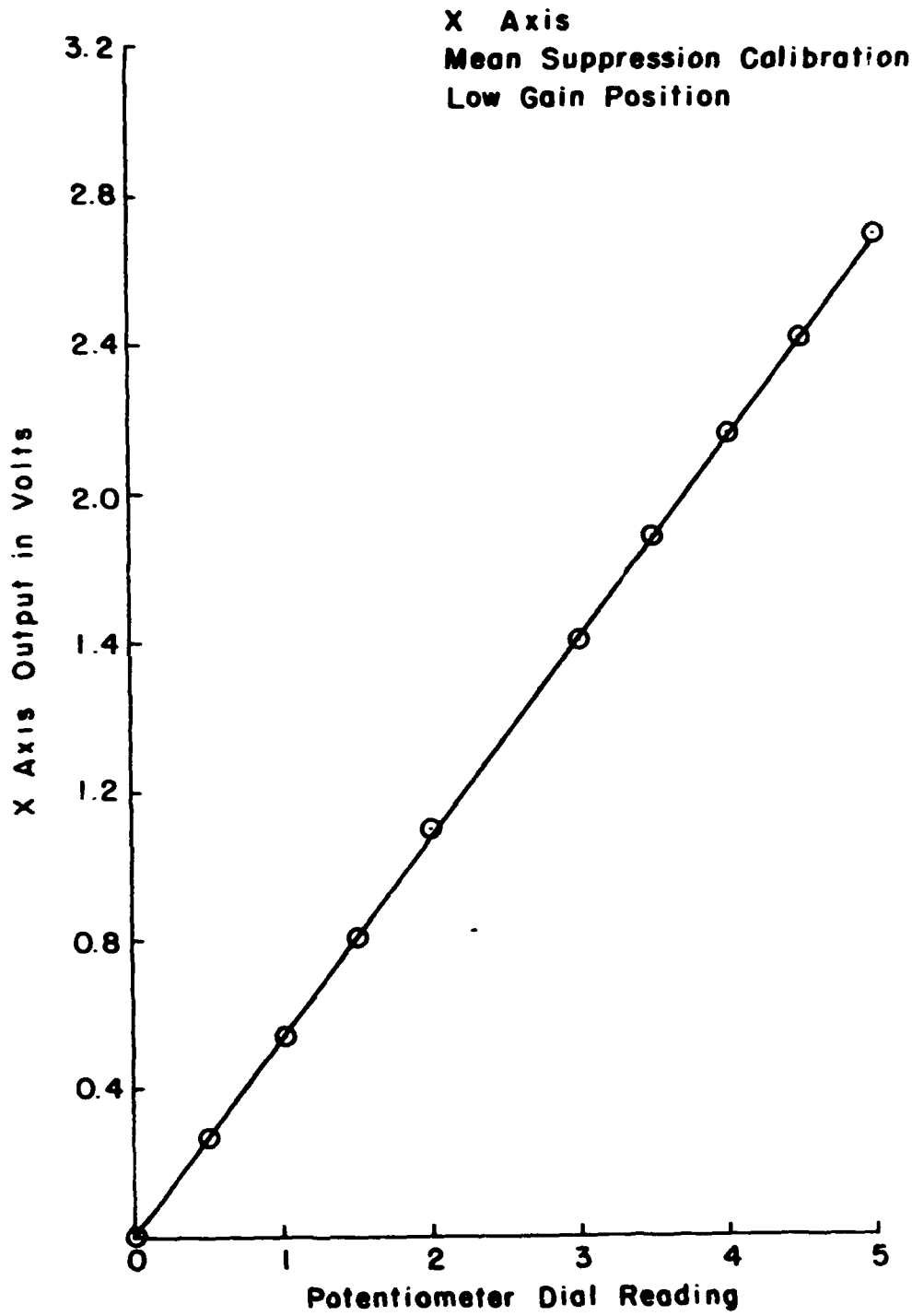

Figure 3.7. Mean suppression calibration curve.

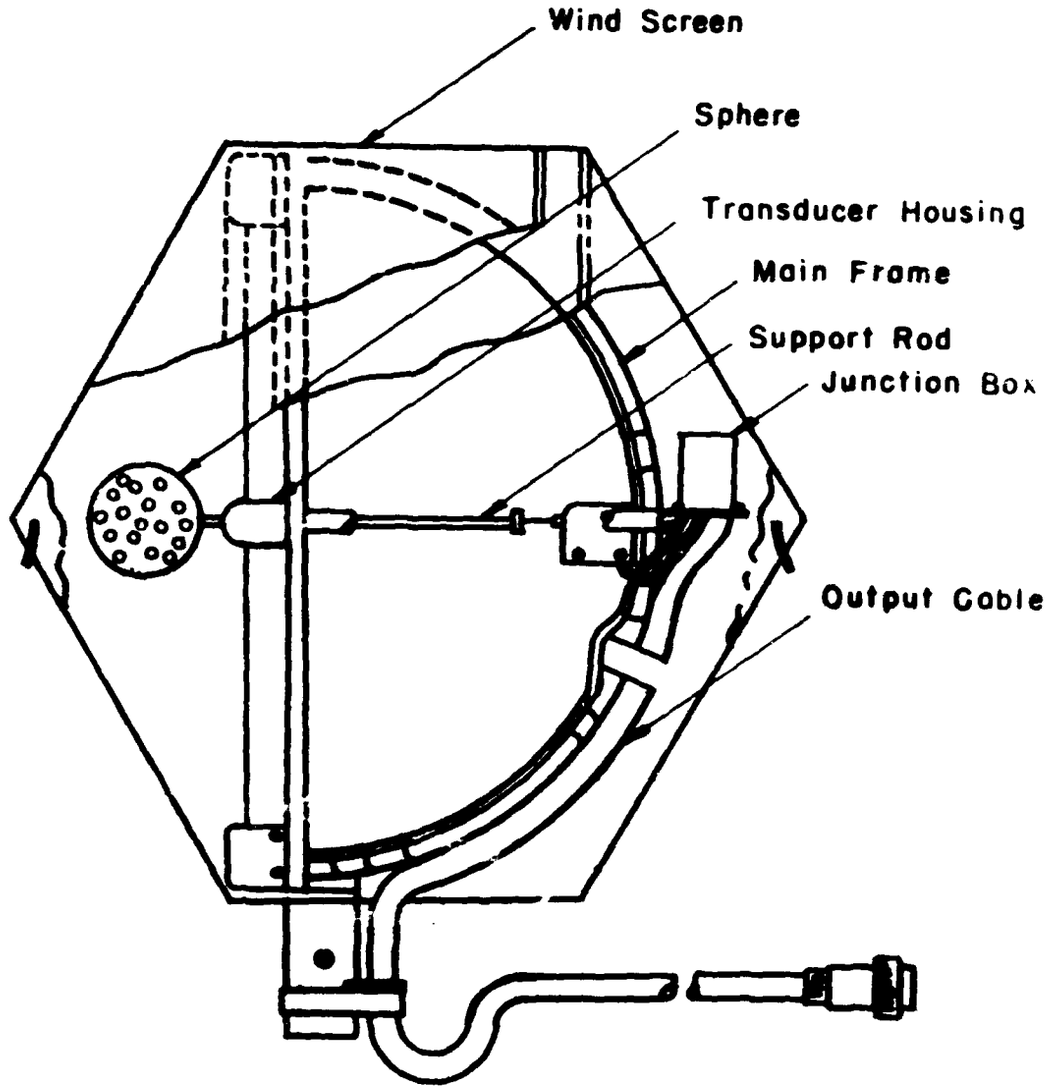

Figure 3.8. Wind unit - outline drawing - original unit.

A small, lightweight, streamlined hood that attaches to the main frame was devised. This hood completely encloses the sensing sphere, and in addition shields the support rods. The hood proved effective in wind tunnel tests up to the maximum test speed at 25 miles per hour. It now remained to build a small test fixture that would display the transducer output voltages at the wind unit so as to allow their adjustment when the wind unit was hooded.

This test fixture was made so that it plugs into the wind unit and the interconnecting cable between wind unit and electronics unit plugs into it. In this way the transducer can be checked and adjusted with the operational set-up essentially intact. The test fixture consists of a battery-operated operational amplifier, with three switch-selectable gains and a sensitive, zero-centered meter. Any of the five transducer output voltages can be selected by a switch, and after suitable amplification displayed on the meter. Since the test jig in no way interrupts normal operation, the operational amplifiers can be checked and adjusted at the same time. In addition, there is a switch position that allows a check on the DC excitation to the transducers. The 6V is passed through a suitable voltage divider so as to be compatible with the 25-0-25 microampere meter movement.

IV. Testing

The testing of the anemometer falls into three general categories; static tests performed in the laboratory and dynamic tests performed in a suitable wind tunnel, and frequency response tests.

The anemometer was first tested statically by hanging laboratory weights along the axes. In this way a plot of output voltage versus force is obtained. This operation tests the linearity of the combined system of springs, dash pots and transducers. A plot of forces versus output voltage is a straight line whose slope is the static calibration constant. This constant is a function of the gain setting of the amplifiers. Each axis was tested in this way and static calibration constants calculated from the plots shown in Figures 4.1, 4.2, and 4.3 which are listed in the following table.

Table of Calibration Constants

	High Gain	Medium Gain	Low Gain
C_X	7.99	13.39	40.83
C_Y	7.68	19.57	39.14
C_Z	7.38	16.2	35.64

All values in gram-meter-sec^{-2} - volt^{-1}

In addition, a test was devised that would determine the ability of the anemometer to resolve a static force into its component parts. A semi-circular frame was constructed so as to complete the hemisphere frame in the horizontal plane. A thread was attached to the junction of the support wires brought out over the semi circular frame and attached to a weight. The thread was brought out over the frame on a knife edge pulley to reduce frictional errors. The frame was marked in degrees from +90 to -90 in five-degree increments. The weight and pulley could then be shifted around the frame so as to simulate the drag force of the windas

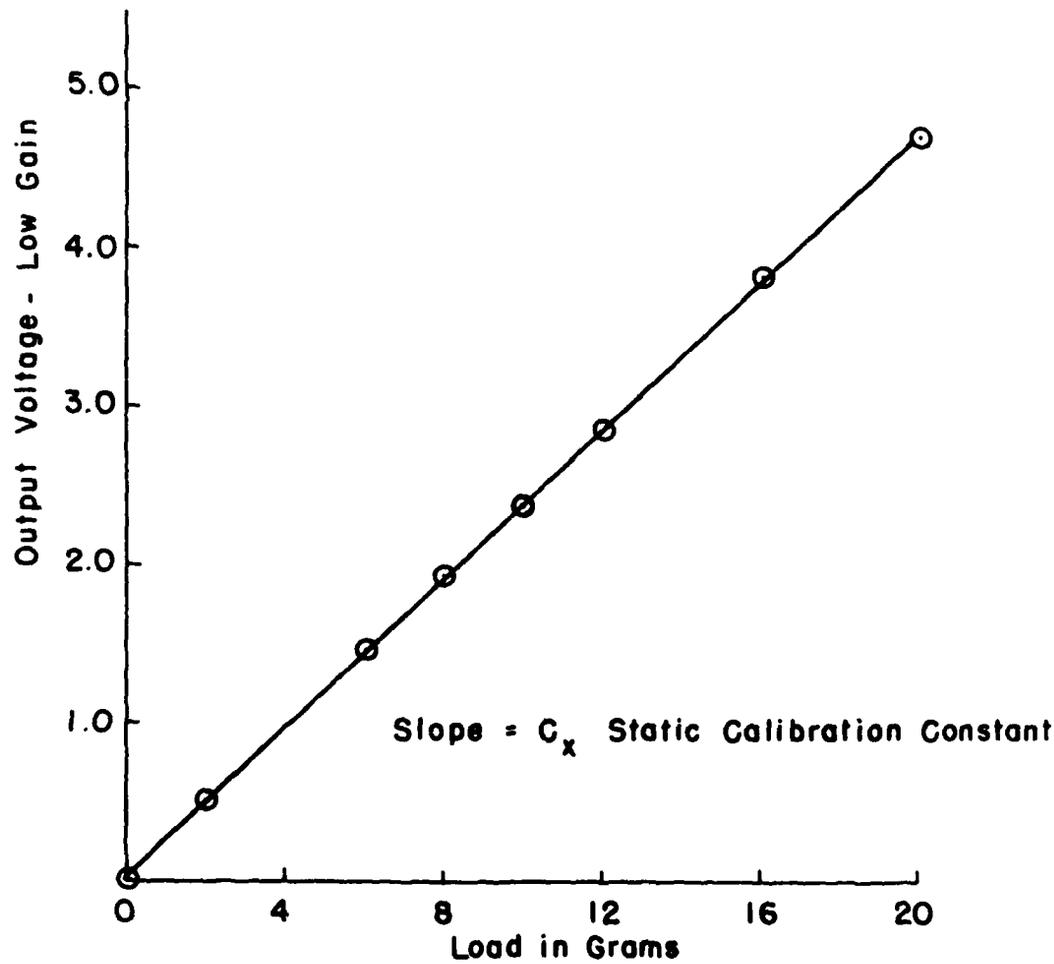

Figure 4.1. Static calibration curve of the X axis.

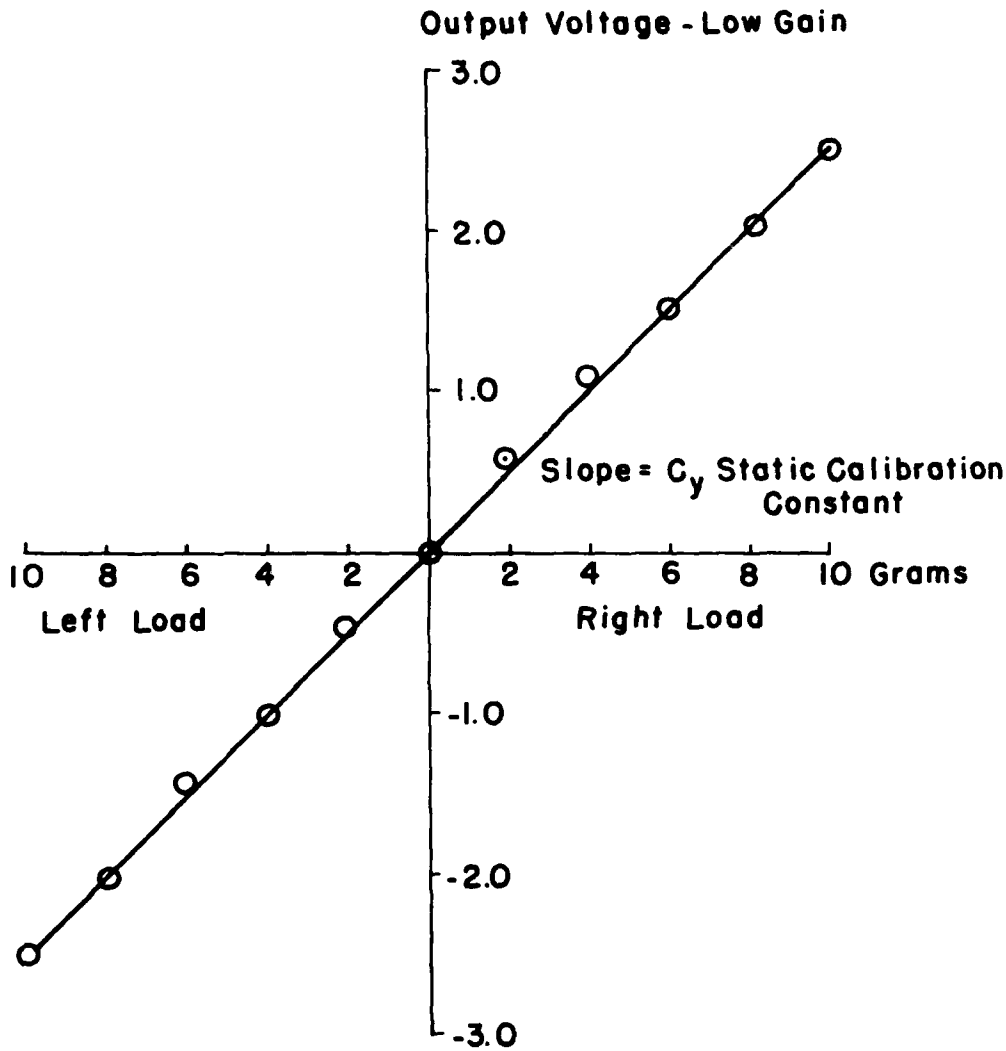

Figure 4.2. Static calibration curve of the Y axis.

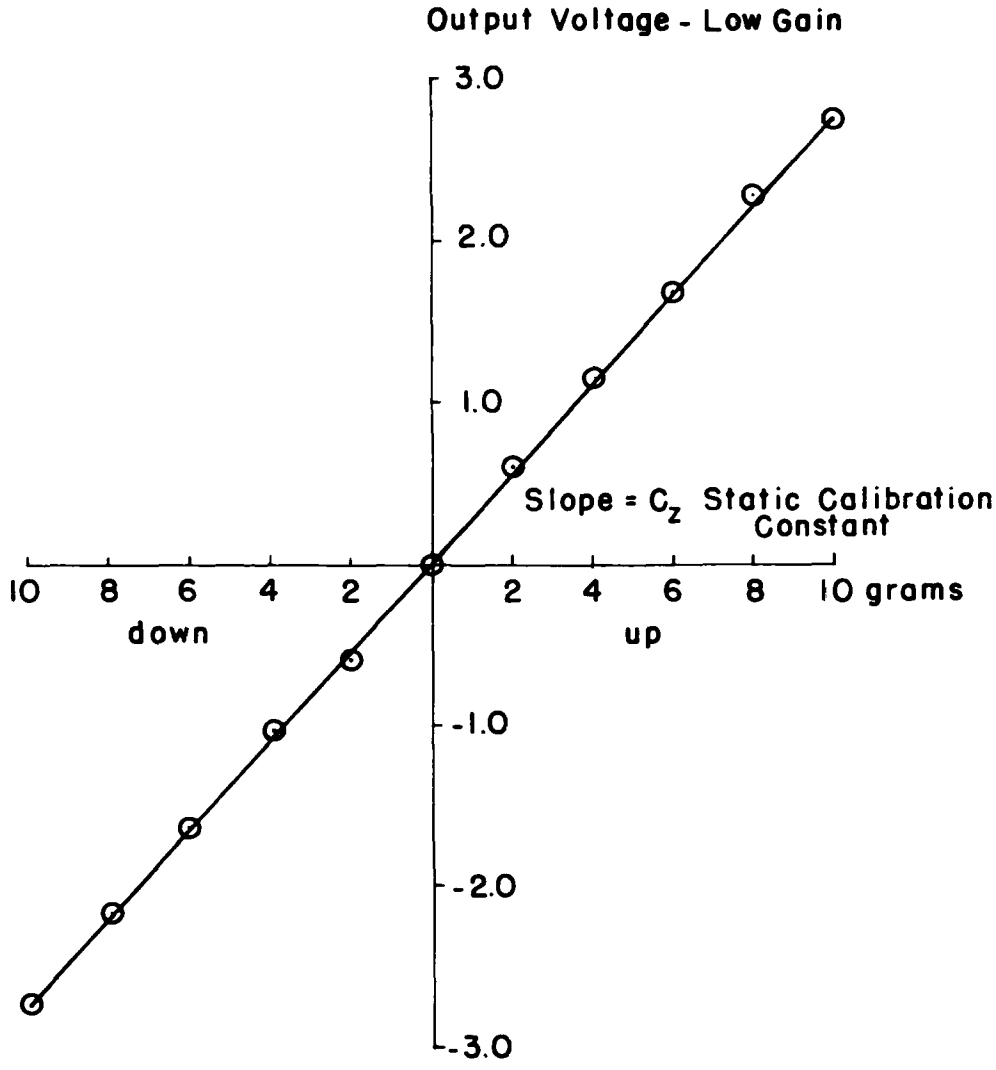

Figure 4.3. Static calibration curve of the Z axis.

its angle of attack varied. The value of component forces were then calculated from the observed voltages and compared to the values obtained using the magnitude of the weight and the azimuthal angle. Figure 4.4 is a plot of theoretical versus observed values as a function of azimuth angle.

The anemometer was then tested in the wind tunnel. The first series of tests were to see how well the instrument obeyed the V^2 law ($\vec{F} = K|\vec{V}|\vec{V}$). The anemometer was placed in the tunnel so that the X axis was coaxial with the wind axis in the tunnel and facing upstream. The tunnel wind speed was then varied from 0 to 25 miles per hour in approximately 2 mile per hour steps. This test was performed twice, February 1968 and April 1968, to see how well the calibration held. The output voltage at each wind speed was recorded and then converted to a force using the static calibration constants obtained in the laboratory. The squared velocity was then plotted against force. The straight line plot thus obtained has a slope K from the relationship; $\vec{F} = K|\vec{V}|\vec{V}$. Figure 4.5 shows the plots obtained and the excellent agreement of both series of tests to the classical V^2 relationship over the entire range of velocities. Since the slope of this plot yields K, the dynamic constant, and since $K = \frac{1}{2} A C_D$; the value of the drag coefficient C_D, of the sphere, can be obtained knowing the constants ρ and A. C_D for the sphere used is 0.617.

Following the V^2 tests, a rotation test was performed to determine the anemometers ability to resolve the vector wind into its components. The anemometer was mounted on a spindle through the floor of the tunnel equidistant from the side walls of the tunnel. The spindle was then rotated manually and the angle of rotation was read from a scale attached to the base

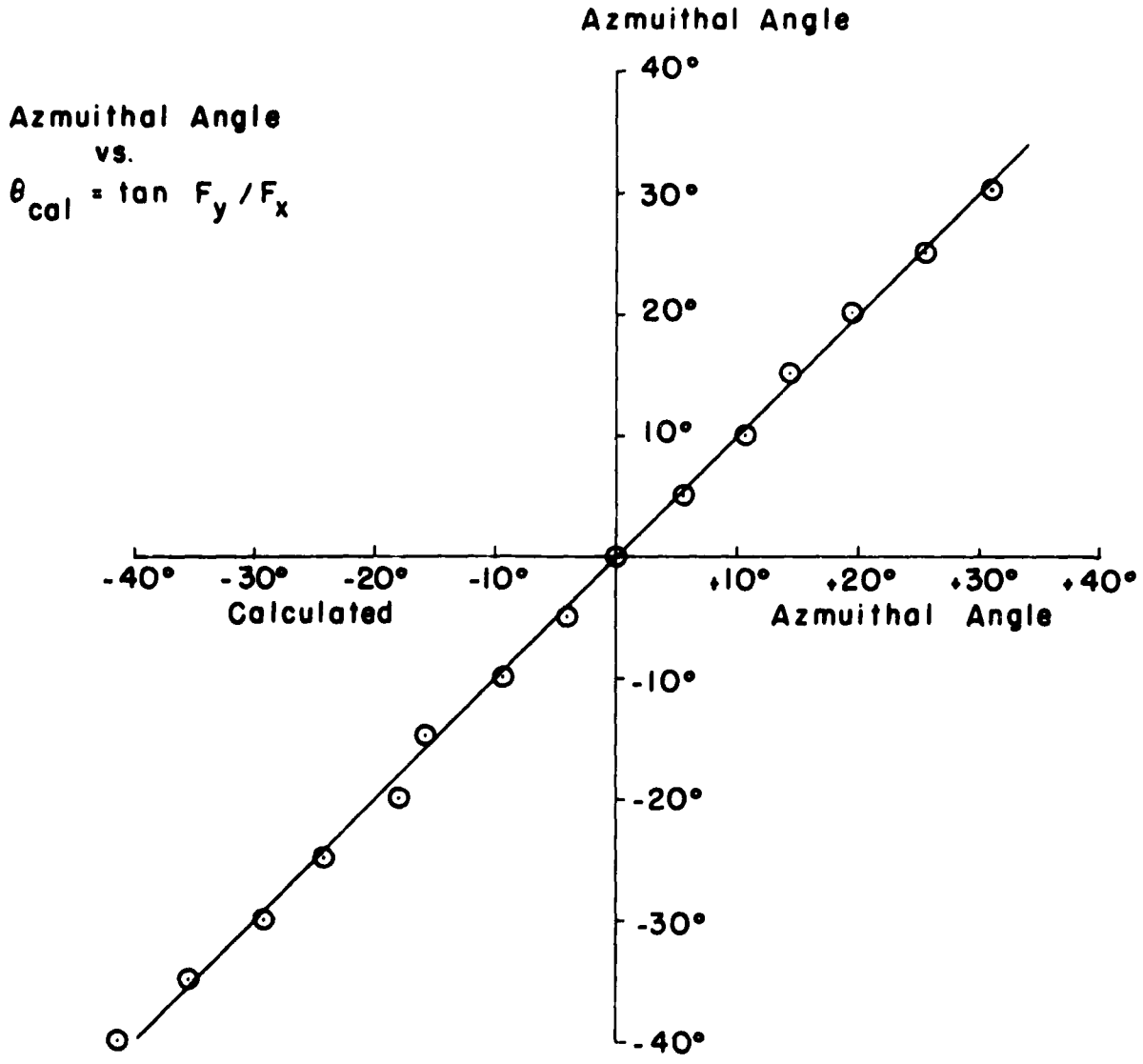

Figure 4.4. Static rotation test - 20 gram load.

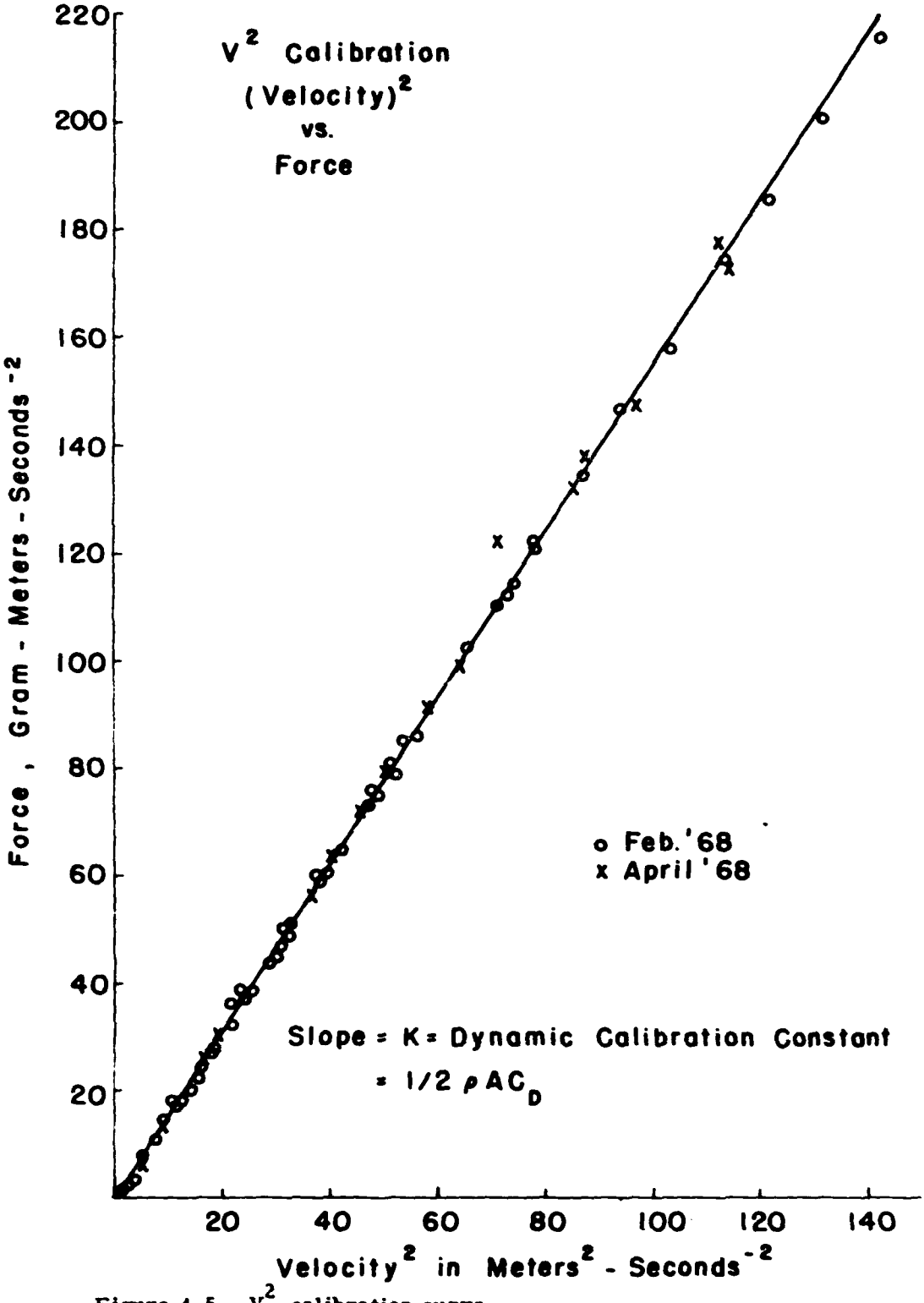

Figure 4.5. V^2 calibration curve.

of the spindle. This scale was marked every two degrees. The anemometer was first aligned so that the X axis was coaxial with the tunnel axis and pointing upstream. The spindie was then rotated $\pm$ 45° (CW and CCW, when viewed from above) from its initial position. The wind velocity (obtained from a pilot static tube) and anemometer voltage outputs were read at each angular position. The test was repeated at three wind speeds 10, 15 and 20 miles per hour. From the data the magnitude of the wind velocity was calculated and compared with the value obtained from the pilot-static tube. The azimuthal angle was also calculated and compared with the actual value read from the scale.

The magnitude of $\vec{V}$ is calculated in the following manner:

Since

$$\vec{F} = K|\vec{V}|\vec{V},$$

then

$$|\vec{V}| = [\,|\vec{F}|/K]^{\frac{1}{2}}, \text{ and}$$

$$|\vec{F}| = [F_x^2 + F_y^2 + F_z^2\,]^{\frac{1}{2}}.$$

Here

$$F_x = C_x e_x,$$

$$F_y = C_y e_y, \text{ and}$$

$$F_z = C_z e_z = 0 \text{ for this test.}$$

Thus,

$$|\vec{V}| = \left[\frac{[(C_x e_x)^2 + (C_y e_y)^2]^{\frac{1}{2}}}{K} \right], \text{ and}$$

e_x = voltage output of the x axis, and

e_y = voltage output of the y axis.

The azimuthal angle θ, is calculated in the following manner:

$$\theta = \tan\left\{\frac{F_y}{F_x}\right\} = \tan^{-1}\left\{\frac{C_y e_y}{C_x e_x}\right\}$$

The results of the rotation test were very disappointing. Large errors in the calculated azimuthal angle were noted along with large errors in the magnitude. Thus, the anemometer showed a marked inability to resolve the wind into components. This result was completely at odds with the results of the static resolution of force test. There was one major difference in the two tests. In the static tests, the force was applied at the center of action of the wind unit, the junction point of the five support rods. The sphere upon which the drag force is exerted was mounted on a threaded rod which screwed into the junction of the support rods. When the sphere was firmly in place its center was approximately 1.5 inches from the junction point (see Figure 3.4). Thus, the drag force was acting through a moment arm. The moment effect was felt only in the transverse and vertical components and therefore its effect was a function of the angle of attack of the wind. In order to correct this effect, the sphere was moved so that its center was coincident with the junction point of the support rods (see Figure 4.6).

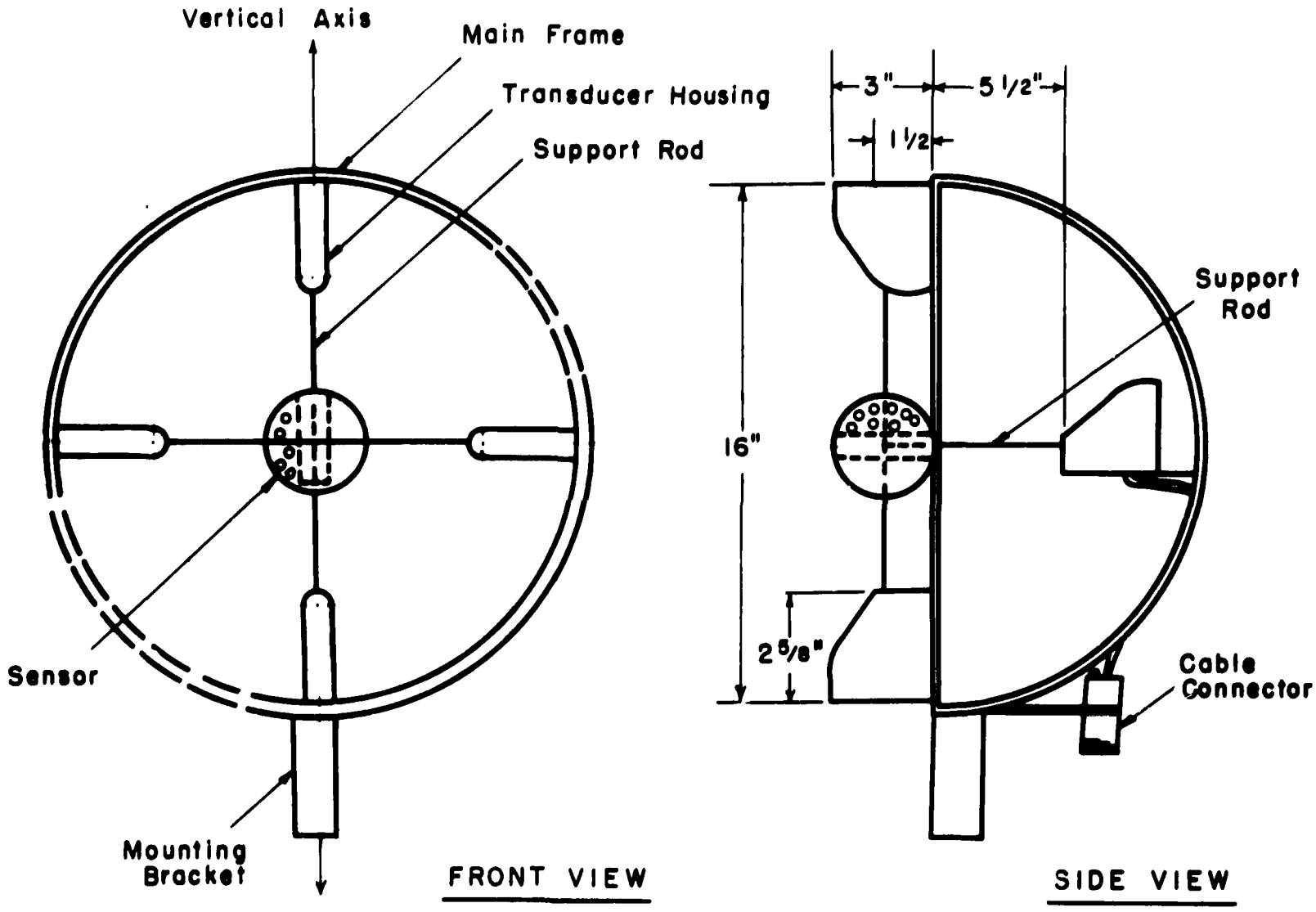

Figure 4.6. Wind unit - outline drawing.

It was feared that moving the sphere into the center might cause a serious deterioration in the vector resolution as the angle of attack increased. The results of the rotation tests performed after the sphere was moved are shown plotted in Figures 4.7 through 4.12. The results show these fears to be groundless. For azimuthal angles θ of ± 20 the maximum error is 2°, and for θ of $\pm 40°$ this error increases to a maximum of 4°. The errors in magnitude in the range $\theta = \pm 20°$ are seen to be 4% maximum, and reach a maximum of 6% as θ is increased to $\pm 40°$.

The final test performed was the step response test which was used to ascertain the frequency response of the instrument. The test is a simple one. A weight is suspended by a thread from the sensing sphere. The weight represents a fixed static load. The supporting thread is then burned so as to almost instantaneously remove the load thus creating a near step input to the anemometer. The output voltages are recorded during this test. Thus, the input and output functions are known and the transfer or response characteristics of the anemometer can be determined. It should be pointed out that the transfer function thus determined is for a step input of force. Since the anemometer responds to the velocity squared ($F = KV^2$) the transfer function unfortunately does not apply for wind.

This test was performed both before and after the addition of silicon oil to the dash pots. The output recordings taken when there is no dash pot fluid clearly indicate the natural frequency of the system, 33.3 hertz in this case. By varying the viscosity of the dash pot fluid and noting the change in the output, the proper viscosity can be chosen so as to bring the unit to

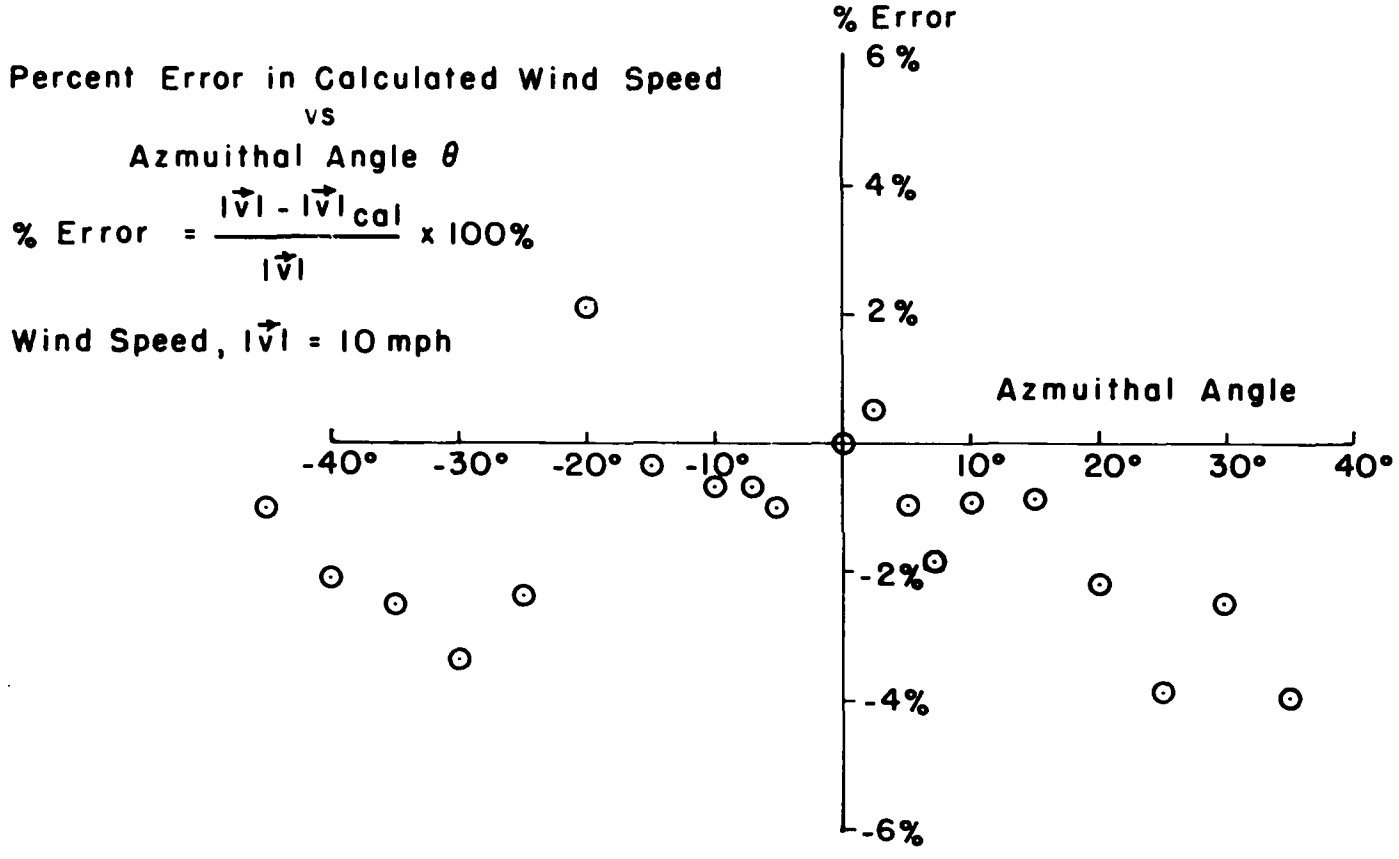

Figure 4.7. Rotation test 10 mph. Magnitude error.

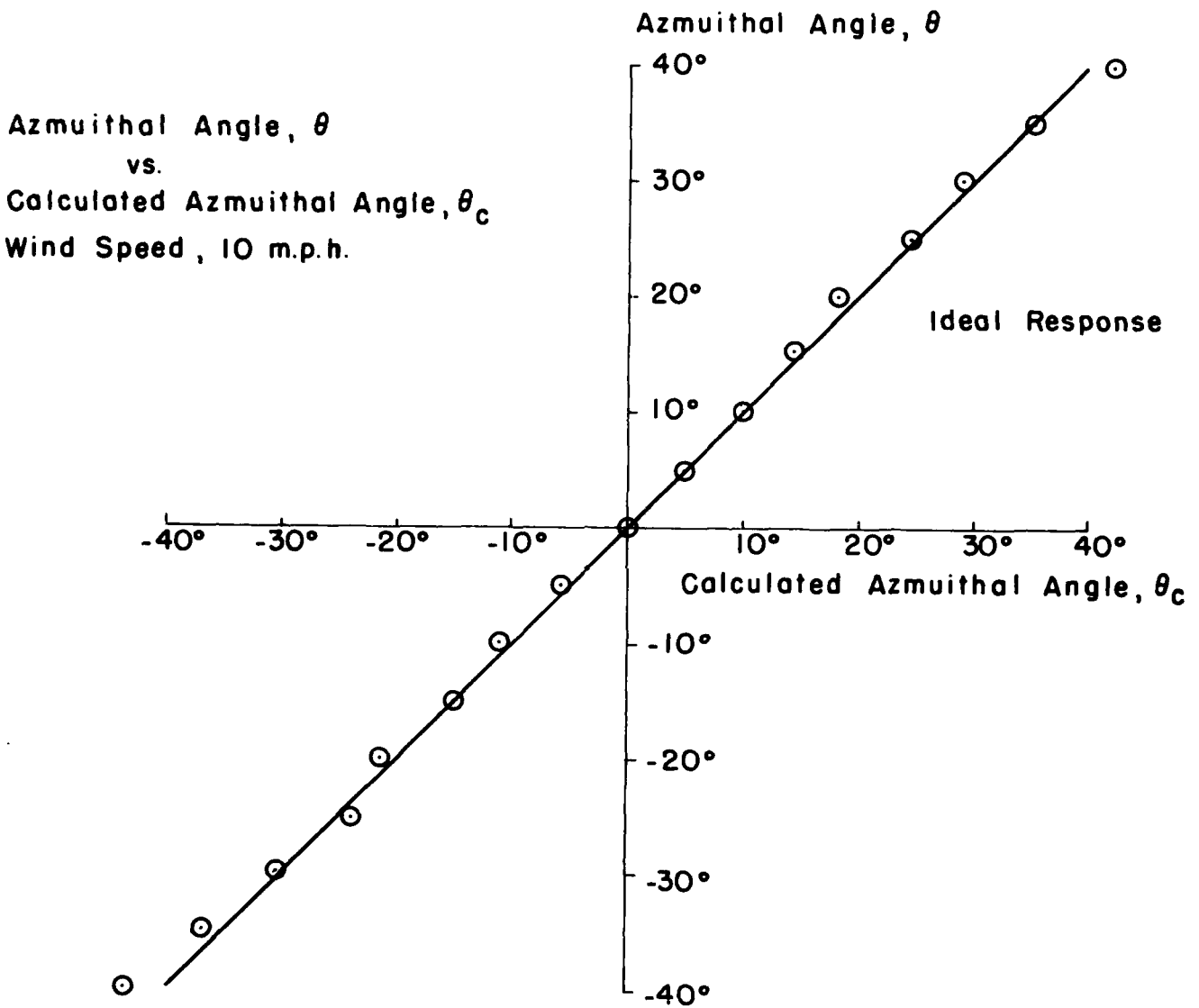

Figure 4.8. Rotation test 10 mph. Angular error.

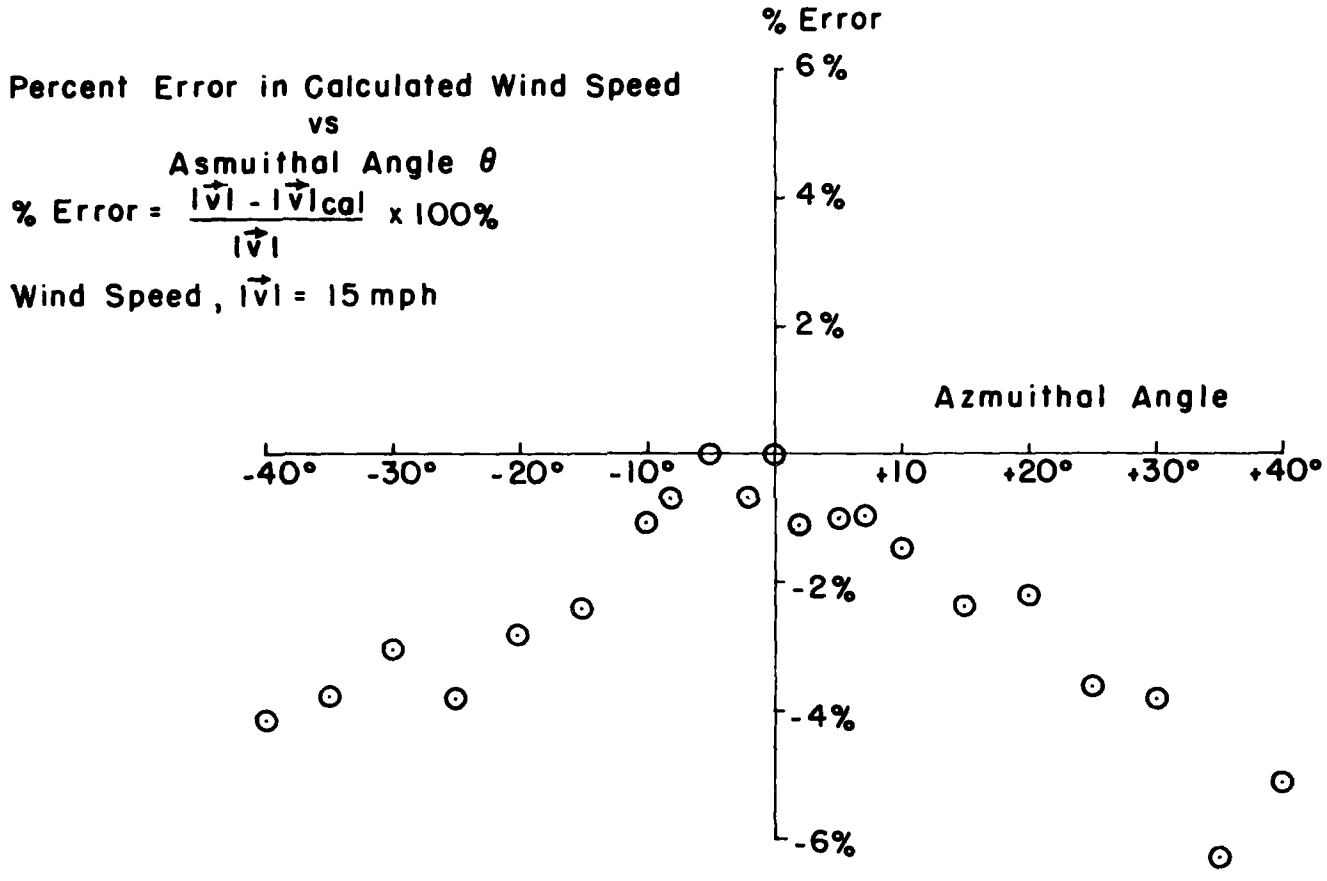

Figure 4.9. Rotation test 15 mph. Magnitude error.

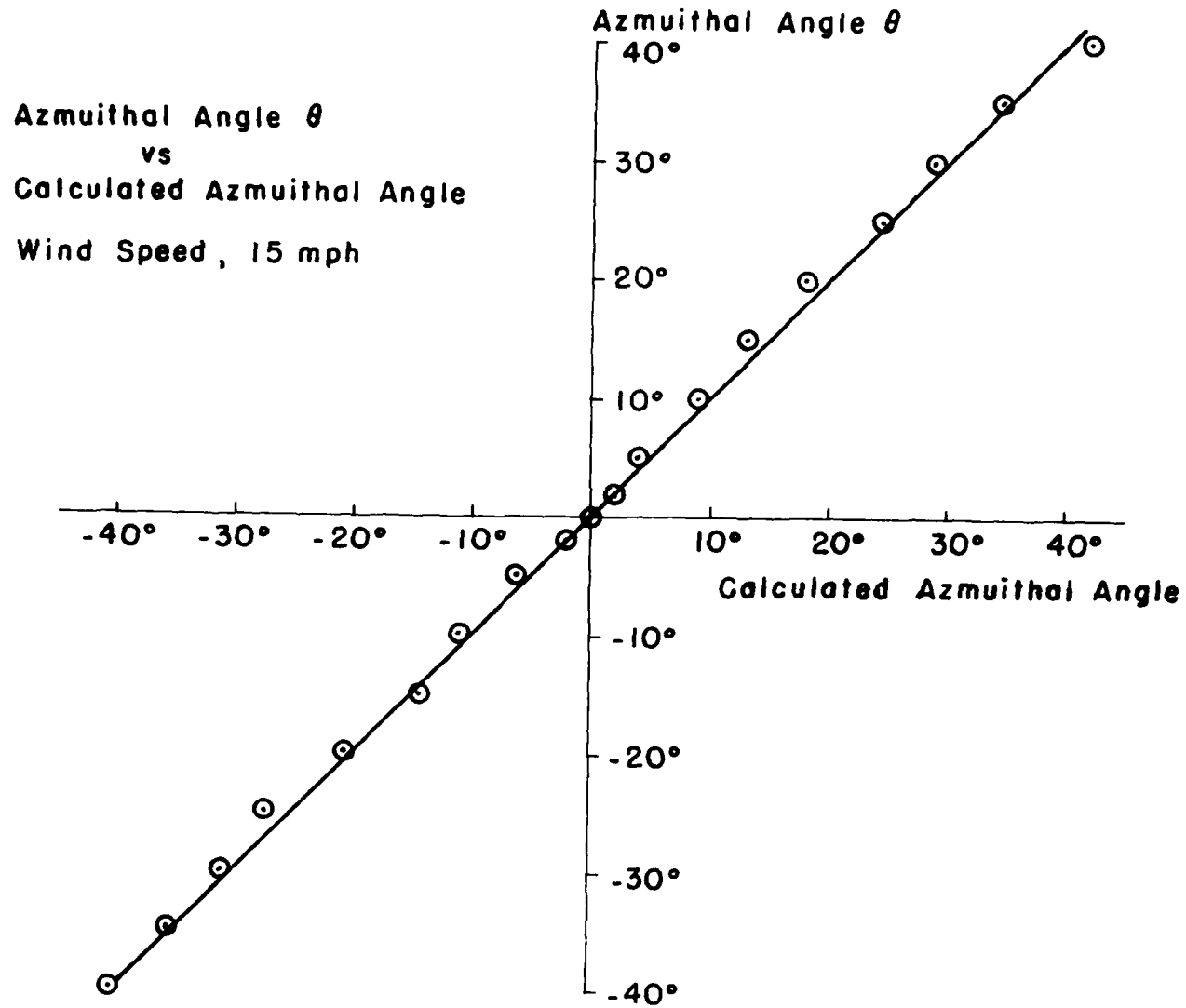

Figure 4.10. Rotation test 15 mph. Angular error.

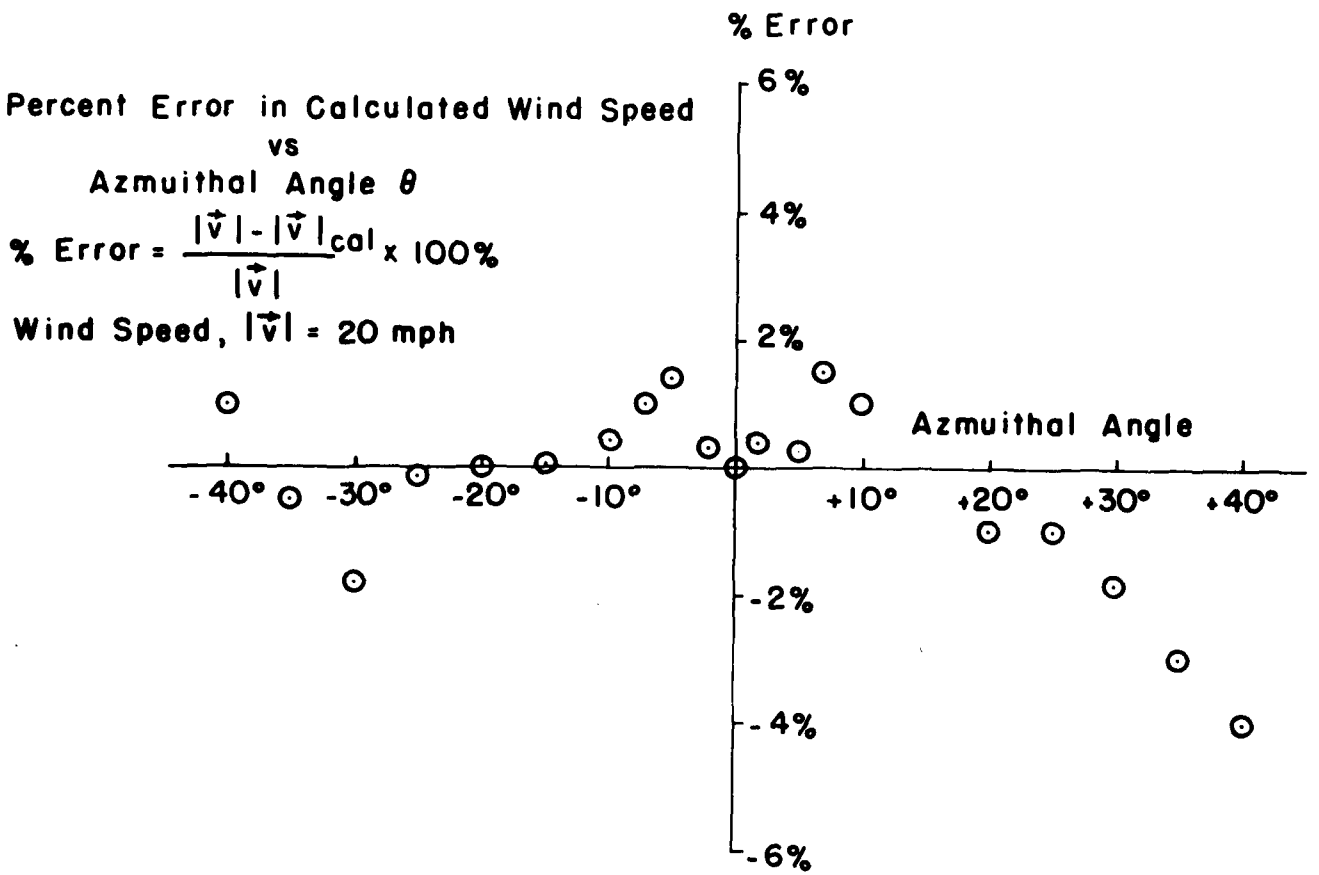

Figure 4.11. Rotation test 20 mph. Magnitude error.

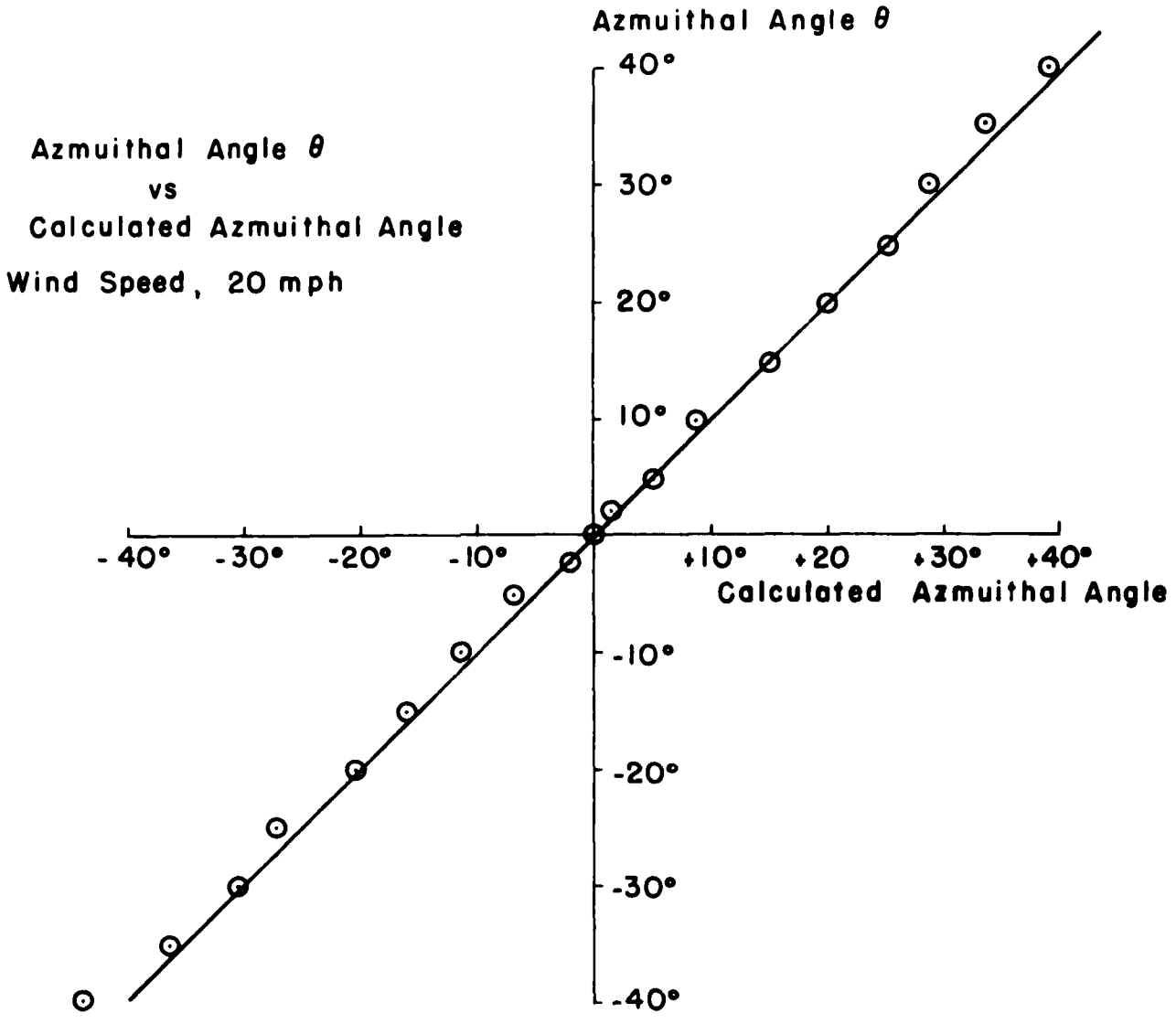

Figure 4.12. Rotation test 20 mph. Angular error.

approximately 0.7 critical damping thus optimizing the response function.

The anemometer was tilted so that the load acts on all three axes and the step response of all three axes can be simultaneously recorded on the Brush Model 260 chart recorder. Three sets of outputs are displayed in Figures 4.13, 4.14a and 4.14b.

Figure 4.13 is the record of the output voltages of three axis when the step is applied and there is no damping fluid in the dash pots. This test was performed to ascertain the natural frequency of the mechanical system consisting of the sensing sphere, springs and dash pots. The chart speed during this record was 125 m/sec, thus, each division (5 mm) is 40×10^{-3} seconds. Eight oscillations occur in 6 divisions or 240×10^{-3} seconds. Thus, the natural frequency, f_n, of the mechanical system is 33.3 hertz.

Figure 4.14 is the record of the step response after the addition of Dow Corning type 200 silicon oil to the dash pots. An oil with a viscosity of 25,000 center stroke was used for this test. This record shows this system to be overdamped. The response times are approximately 2.5 divisions or 100×10^{-3} seconds, which would allow measurements up to 10 hertz.

The dash pot fluid was then made less viscous and after several attempts; the response shown in Figure 4.15 was achieved. In this test a 15,000 centerstroke oil was used in the X axis dash pot and a 12,500 centerstroke oil in the Y and Z dash pots. Again each major division on the chart record is 40×10^{-3} sec.

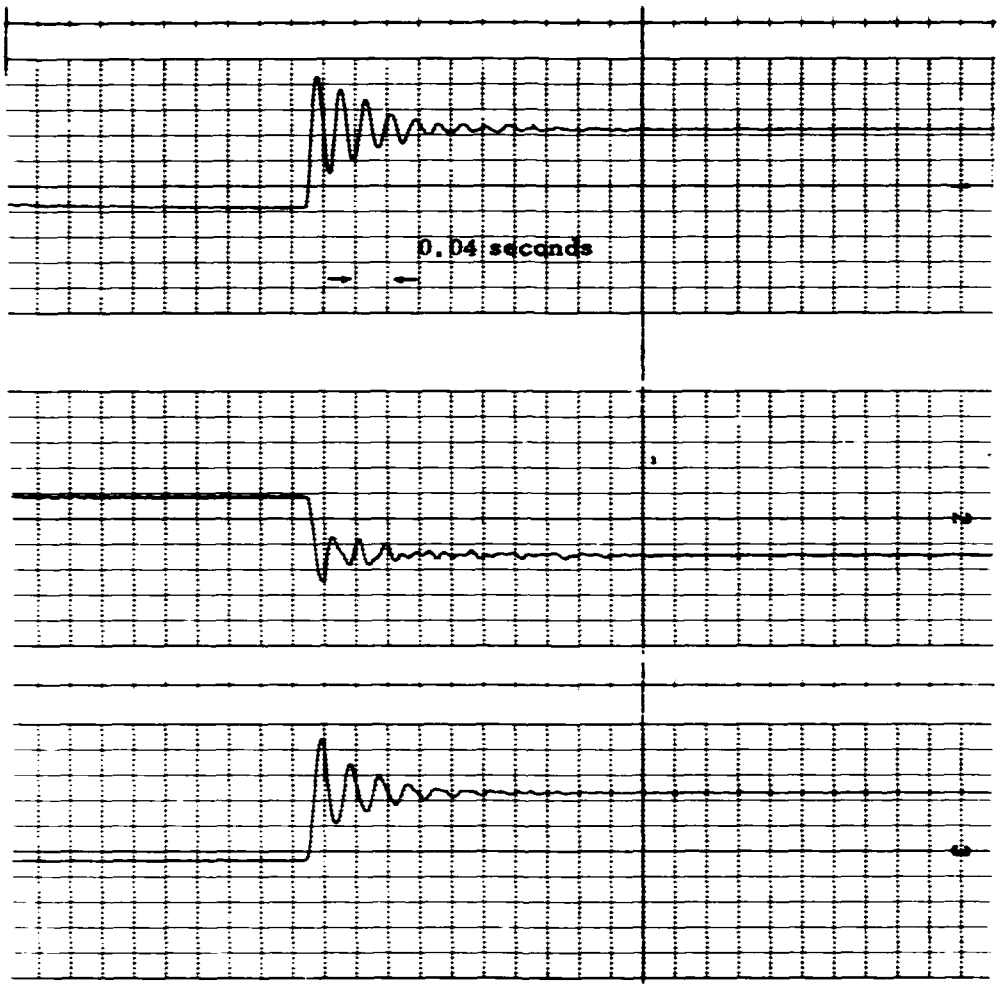

Figure 4.13. Underdamped response. Chart recordings of the output voltages of X, Y and Z axis (1, 2 and 3 respectively) resulting from a "step input".

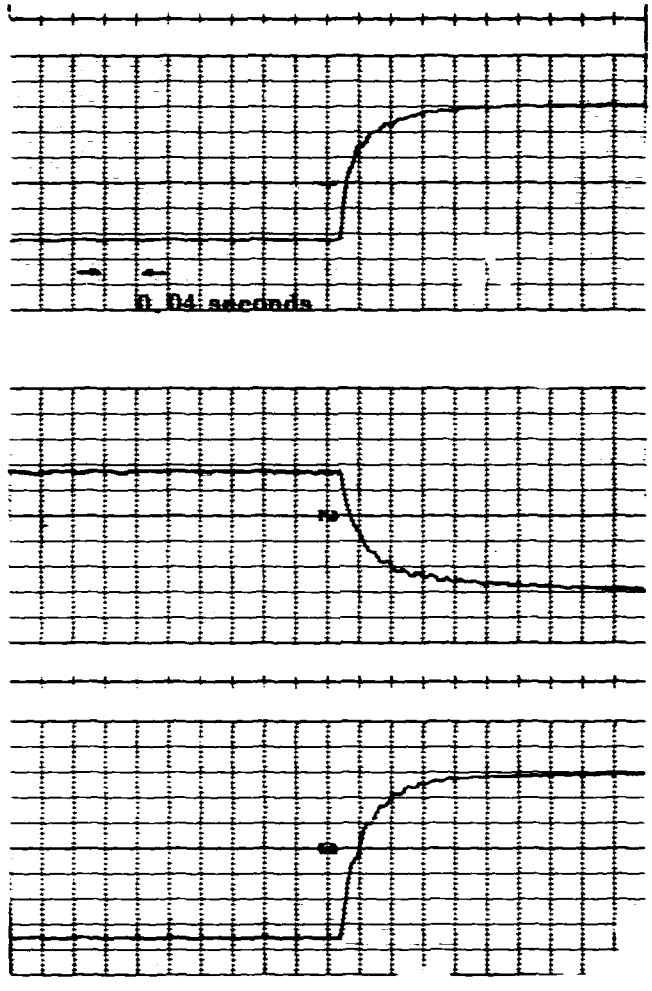

Figure 4.14. Overdamped response. Chart recordings of the output voltages of the X, Y and Z axis (1, 2 and 3 respectively) resulting from a "step input".

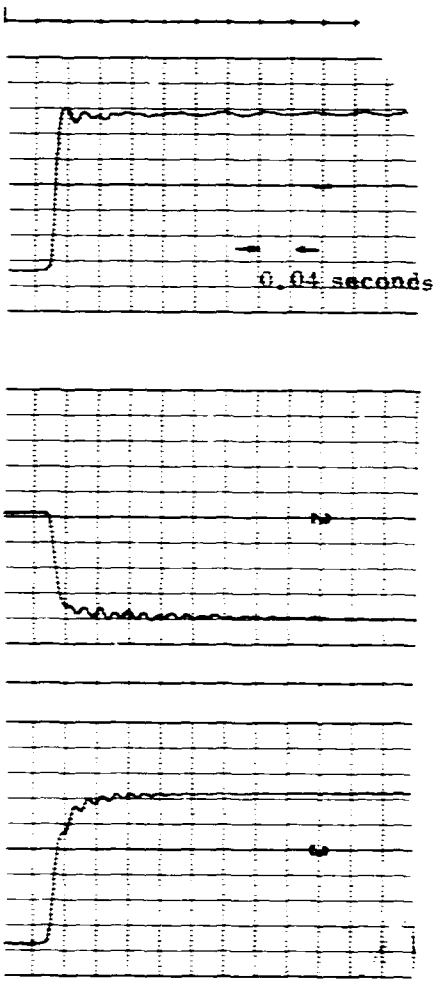

Figure 4.15. Optimized response. Chart recordings of the output voltages of the X, Y and Z axis (1, 2 and 3 respectively) resulting from a step input.

The X axis is still slightly underdamped with an overshoot of 1 part in 30. Using the relationship

$$\gamma = \sqrt{\frac{1}{[\log_e \pi / a/A)]^2}} + 1 \qquad \text{(Doebelin, 1966)}$$

where

γ = coefficient of damping

and

a/A = overshoot

The X axis was found to be 0.78 critically damped. This assures a flat response to 10 hertz.

The Y and Z axes are seen to be still slightly overdamped; that is $\gamma > 1$. However, the rise time (time necessary to reach 0.9 of its final value) is only 30×10^{-3} seconds. This response will also allow measurements to 30 hertz. Thus, all three axes are capable of measuring to 10 hertz, which was the design criterion. The data acquisition system used in conjunction with the anemometer in the field includes 11 hertz filtering with a drop off of 18 db/octave. The natural frequency of the mechanical system will thus be attenuated by approximately 25 db.

There is another type of filtering inherent in the anemometer due to the physical dimensions of the sensing sphere (7.8 centimeters diameter) since the sphere would tend to low-pass filter those eddies equal in size or smaller then itself. The relationship between the mean wind and the cutoff frequency and dimensions of the sensing sphere was reported by Kirwan,

et al., (1966) and is

$$f_{cutoff} = \bar{u}\ 7.8 \quad \text{(Hinze, 1959)}$$

For example, when $\bar{u}$ is 2 meters/second, the cutoff frequency will be approximately 25 hertz which is considerably higher than the 10 hertz required.

Figure 4.16 show the results of tests designed to obtain some figure of merit of the noise content of the anemometer and data acquisition system. Figure 4.15a is the output of the X-axis under the influence of a 20 mile per hour in the wind tunnel. This record was made at a chart speed of 125 mm/second and a sensitivity of 125×10^{-3} volts 1 mm. The data was not filtered during these tests. A mean voltage of 9 volts resulting from the mean speed was "backed out" using the mean suppression circuit and the highest gain setting then used. The perturbations shown are thus about 0 volts. Figure 4.15b was made with no wind in the tunnel, no mean suppresion, at the same chart speed but with the sensitivity now at 5×10^{-3} volts/mm. That there is very little if any inherent noise in the system is obvious from this record.

Figure 4.15c is the record obtained again with an 20 mile per hour wind but with the instrument now hooded. The sensitivity is again 125×10^{-3} volts/mm and the chart speed is again 125 mm/second. There is no mean suppression and the gain is again in the high position. This signal thus represents a zero centered noise signal. However, it is quite small in amplitude compared with the 9 volt mean signal that the hood is suppress-

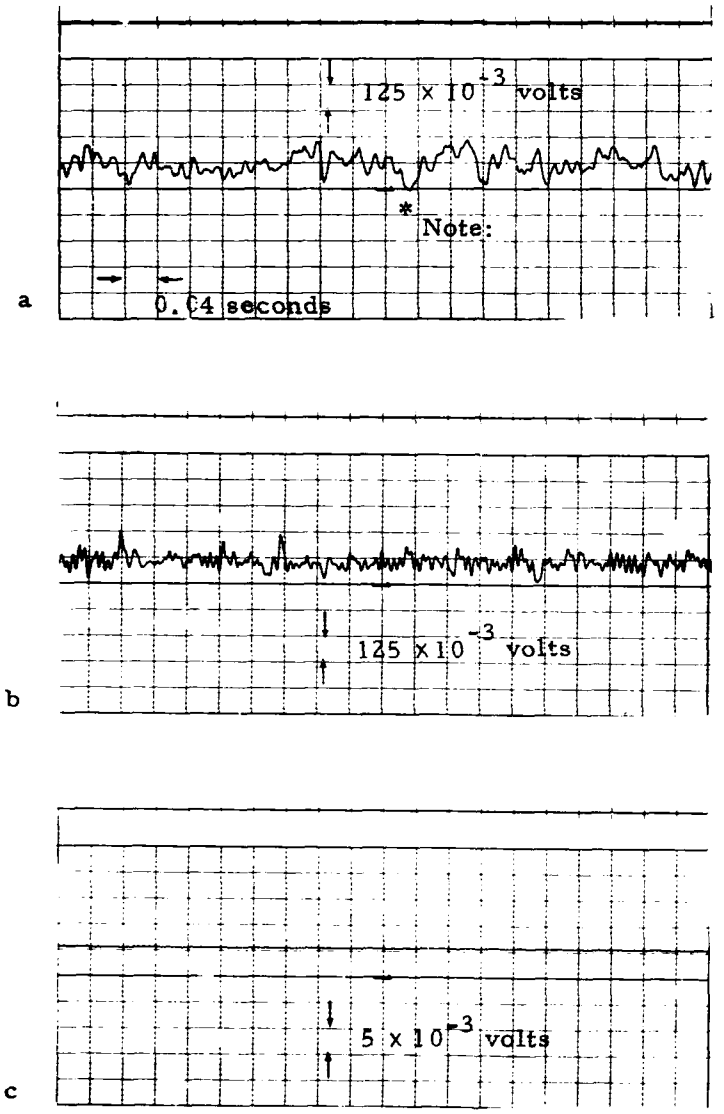

Figure 4.16. Noise output, chart recordings of the X axis output voltage with a) 20 mph wind b) 20 mph wind with the instrument hooded and c) no wind

*Note: Perturbations about a mean signal of 9 volts.

ing, and its frequency content is much higher than that observed when the instrument was not hooded. This suggests the signal really is produced by some form of vibration induced by the hood.

V. Conclusions

This instrument has been demonstrated through the results of both the static and dynamic tests to be superior to the original thrust anemometer. It is capable of measuring wind speeds to 25 miles per hour and resolving the vector wind into its magnitude, azimuthal, and elevation angles with an accuracy in magnitude of better than 4% and an angular resolution of 2°. It has the necessary frequency response to allow measurements in the range of DC to 10 hertz. In addition, its field operation has been greatly simplified with the addition of a hood and calibration test jig.

The thrust anemometer has two major drawbacks in field operations. First, the anemometer requires an absolutely stable platform. Any instabilities in the platform are translated to output signals because of inertial effects and the instruments sensitivity to orientation. Its sensitivity to orientation stems from the weight of the sensing sphere (10 grams) which is totally supported by the z (vertical) axis when the instrument is level. Any change in level causes some part of this 10 grams to be shifted to either the Y or Z axis or both depending on how it is misoriented. This effect goes as the sine of angle of rotation from level.

The second problem is the inability to re-zero the anemometer after it has been installed in the field due to the remote location of the wind unit. If the anemometer is used as it was on a tower and a ship as the base of

operation, the problem is compounded since the zeroing cannot be done on the ship either. The hood and test jig discussed in Section IV offer the solution to this second problem and might offer some degree on the first problem also. If instabilities are noted in the anemometer mount then a second hooded instrument could serve to give the data necessary to correct the wind data from the first unit for inertial and misorientation errors. This might be best done after the data has been reduced. That is to treat the hooded instrument's data as wind data and carry through the data reduction so as to construct u, v, and w spectra and use these spectra to correct the u, v, and w spectra obtained from the unhooded instrument. The hooded wind tunnel tests show that the hooding does not seem to induce any noise in the frequency range of interest. The self induced noise seems to be a much higher frequency.

In conclusion, the results of laboratory and wind tunnel tests are most encouraging. However, the final evaluation of the thrust anemometer as a useful turbulence anemometer is an air-sea interaction program must be accomplished in future field tests.

Acknowledgements:

The anemometer described here was completely fabricated at New York University under Contract No. 285(57). The author is deeply indebted to the painstaking efforts of Mr. Louis Amelio on the construction of the wind units and Mr. Joel Katz for construction of the electronics unit. In addition, the author wishes to thank Professor A.D. Kirwan, Jr. for his patience, Mrs. Lillian Bloom for her careful typing of this manuscript and Mrs. Gertrude Fisher for her work in finishing the illustrations.

References

Doe, L.A.E., 1963: A three-component thrust anemometer for studies of vertical transports above the sea surface. Ph.D. Thesis, Department of Meteorology and Oceanography, New York University (unpublished manuscript).

Doebelin, E.O., 1966: Measurement Systems: Application and Design. McGraw-Hill Book Co., New York.

Kirwan, A.D., Jr., S. Adelfang, G.J. McNally, 1966: Laboratory and field evaluation of thrust anemometer. Geophysical Science Report No.66-10, New York University (unpublished manuscript).

Miyake, M., 1967: A constant temperature wind component meter and its performance characteristics. J. of Appl. Meteor., Vol.6, pp. 186-194.

Pandolfo, J., 1960: Power spectrum analyses of turbulent surface winds over water under inversion conditions. Tech. Report under Contract Nonr 285(03), Department of Meteorology and Oceanography, New York University (unpublished manuscript).

Pond, S., R.W. Stewart and R.W. Burling, 1963: Turbulence spectra on wind over waves. J. Atmos. Sci., Vol.20, p. 319.

Smith, S.D., 1966: Thrust anemometer measurements of wind velocity fluctuations spectra and stress over the sea. Report B10-66-B, Bedford Institute of Oceanography, Dartmouth, N.S. (unpublished manuscript).

Unclassified

Security Classification

DOCUMENT CONTROL DATA - R&D

(Security classification of title, body of abstract and indexing annotation must be entered when the overall report is classified)

1. ORIGINATING ACTIVITY (Corporate author) New York University, Research Division School of Engineering and Science	2a. REPORT SECURITY CLASSIFICATION Unclassified 2b. GROUP

3. REPORT TITLE

A Thrust Anemometer for the Measurement of the Turbulent Wind Vector

4. DESCRIPTIVE NOTES (Type of report and inclusive dates)

Scientific Report

5. AUTHOR(S) (Last name, first name, initial)

Gerard J. McNally

6. REPORT DATE	7a. TOTAL NO. OF PAGES	7b. NO. OF REFS
January 1970	43+v	7

8a. CONTRACT OR GRANT NO.	9a. ORIGINATOR'S REPORT NUMBER(S)
Nonr 285(57) b. PROJECT NO. 1103 c. d.	GSL-TR-70-1 9b. OTHER REPORT NO(S) (Any other numbers that may be assigned this report)

10. AVAILABILITY/LIMITATION NOTICES

Qualified requesters may obtain copies of this report from DDC.

11. SUPPLEMENTARY NOTES	12. SPONSORING MILITARY ACTIVITY

13. ABSTRACT

An improved version of a three component thrust anemometer is discussed in this paper. The design criteria and specifications of its component parts are outlined. Results of laboratory and wind tunnel tests are described which were designed to test the static characteristics and frequency response of the anemometer as well as results of wind tunnel tests. These tests demonstrate the anemometers adherence to the V^2 law ($\vec{F} = K\,\vec{V}|\vec{V}|$) over the velocity range 0 to 25 miles per hour. Rotation tests performed at various wind speeds provide information on the anemometer's ability to resolve the vector wind into its components.

DD FORM 1 JAN 64 1473

Unclassified

Security Classification

Unclassified

Security Classification

14 KEY WORDS	LINK A		LINK B		LINK C	
	ROLE	WT	ROLE	WT	ROLE	WT
anemometer						
turbulence						
vector wind						
drag sphere						

INSTRUCTIONS

1. **ORIGINATING ACTIVITY:** Enter the name and address of the contractor, subcontractor, grantee, Department of Defense activity or other organization *(corporate author)* issuing the report.

2a. **REPORT SECURITY CLASSIFICATION:** Enter the overall security classification of the report. Indicate whether "Restricted Data" is included. Marking is to be in accordance with appropriate security regulations.

2b. **GROUP:** Automatic downgrading is specified in DoD Directive 5200.10 and Armed Forces Industrial Manual. Enter the group number. Also, when applicable, show that optional markings have been used for Group 3 and Group 4 as authorized

3. **REPORT TITLE:** Enter the complete report title in all capital letters. Titles in all cases should be unclassified. If a meaningful title cannot be selected without classification, show title classification in all capitals in parenthesis immediately following the title.

4. **DESCRIPTIVE NOTES:** If appropriate, enter the type of report, e.g., interim, progress, summary, annual, or final. Give the inclusive dates when a specific reporting period is covered.

5. **AUTHOR(S):** Enter the name(s) of author(s) as shown on or in the report. Enter last name, first name, middle initial. If military, show rank and branch of service. The name of the principal author is an absolute minimum requirement.

6. **REPORT DATE:** Enter the date of the report as day, month, year, or month, year. If more than one date appears on the report, use date of publication.

7a. **TOTAL NUMBER OF PAGES:** The total page count should follow normal pagination procedures, i.e., enter the number of pages containing information.

7b. **NUMBER OF REFERENCES:** Enter the total number of references cited in the report.

8a. **CONTRACT OR GRANT NUMBER:** If appropriate, enter the applicable number of the contract or grant under which the report was written.

8b, 8c, & 8d. **PROJECT NUMBER:** Enter the appropriate military department identification, such as project number, subproject number, system numbers, task number, etc.

9a. **ORIGINATOR'S REPORT NUMBER(S):** Enter the official report number by which the document will be identified and controlled by the originating activity. This number must be unique to this report.

9b. **OTHER REPORT NUMBER(S):** If the report has been assigned any other report numbers *(either by the originator or by the sponsor)*, also enter this number(s).

10. **AVAILABILITY/LIMITATION NOTICES:** Enter any limitations on further dissemination of the report, other than those imposed by security classification, using standard statements such as:

(1) "Qualified requesters may obtain copies of this report from DDC."

(2) "Foreign announcement and dissemination of this report by DDC is not authorized."

(3) "U. S. Government agencies may obtain copies of this report directly from DDC. Other qualified DDC users shall request through _____."

(4) "U. S. military agencies may obtain copies of this report directly from DDC. Other qualified users shall request through _____."

(5) "All distribution of this report is controlled. Qualified DDC users shall request through _____."

If the report has been furnished to the Office of Technical Services, Department of Commerce, for sale to the public, indicate this fact and enter the price, if known.

11. **SUPPLEMENTARY NOTES:** Use for additional explanatory notes.

12. **SPONSORING MILITARY ACTIVITY:** Enter the name of the departmental project office or laboratory sponsoring *(paying for)* the research and development. Include address.

13. **ABSTRACT:** Enter an abstract giving a brief and factual summary of the document indicative of the report, even though it may also appear elsewhere in the body of the technical report. If additional space is required, a continuation sheet shall be attached.

It is highly desirable that the abstract of classified reports be unclassified. Each paragraph of the abstract shall end with an indication of the military security classification of the information in the paragraph, represented as *(TS)*, *(S)*, *(C)*, or *(U)*

There is no limitation on the length of the abstract. However, the suggested length is from 150 to 225 words.

14. **KEY WORDS:** Key words are technically meaningful terms or short phrases that characterize a report and may be used as index entries for cataloging the report. Key words must be selected so that no security classification is required. Identifiers, such as equipment model designation, trade name, military project code name, geographic location, may be used as key words but will be followed by an indication of technical context. The assignment of links, roles, and weights is optional

DD FORM 1 JAN 64 1473 (BACK)

Unclassified

Security Classification